The Scanning Mechanism of Eukaryotic Translation Initiation

Alan G. Hinnebusch

Laboratory of Gene Regulation and Development, Eunice Kennedy Shriver National Institute of Child Health and Human Development, National Institutes of Health, Bethesda, Maryland 20892; email: ahinnebusch@nih.gov

Annu. Rev. Biochem. 2014. 83:779–812

First published online as a Review in Advance on January 29, 2014

The *Annual Review of Biochemistry* is online at biochem.annualreviews.org

This article's doi: 10.1146/annurev-biochem-060713-035802

Keywords

translation, initiation, scanning, ribosome, eIFs, tRNA

Abstract

In eukaryotes, the translation initiation codon is generally identified by the scanning mechanism, wherein every triplet in the messenger RNA leader is inspected for complementarity to the anticodon of methionyl initiator transfer RNA (Met-tRNA$_i$). Binding of Met-tRNA$_i$ to the small (40S) ribosomal subunit, in a ternary complex (TC) with eIF2-GTP, is stimulated by eukaryotic initiation factor 1 (eIF1), eIF1A, eIF3, and eIF5, and the resulting preinitiation complex (PIC) joins the 5′ end of mRNA preactivated by eIF4F and poly(A)-binding protein. RNA helicases remove secondary structures that impede ribosome attachment and subsequent scanning. Hydrolysis of eIF2-bound GTP is stimulated by eIF5 in the scanning PIC, but completion of the reaction is impeded at non-AUG triplets. Although eIF1 and eIF1A promote scanning, eIF1 and possibly the C-terminal tail of eIF1A must be displaced from the P decoding site to permit base-pairing between Met-tRNA$_i$ and the AUG codon, as well as to allow subsequent phosphate release from eIF2-GDP. A second GTPase, eIF5B, catalyzes the joining of the 60S subunit to produce an 80S initiation complex that is competent for elongation.

Contents

OVERVIEW

Translation initiation entails decoding of the AUG start codon in messenger RNA (mRNA) by methionyl initiator transfer RNA (Met-tRNA$_i$). This process significantly differs between eukaryotes and bacteria, which has profound implications for translational control. In bacteria, annealing of 16S ribosomal RNA (rRNA) in the small (30S) ribosomal subunit with the Shine–Dalgarno sequence in mRNA places the AUG codon in the ribosomal P site. This interaction is lacking in eukaryotes, in which most mRNAs are translated by a scanning mechanism wherein the small (40S) ribosomal subunit is preloaded with Met-tRNA$_i$ by the GTP-bound form of eukaryotic initiation factor 2 (eIF2)—a GTPase with no counterpart in bacteria—in a reaction promoted by eIF1, -1A, and -5 and the multisubunit eIF3; the resulting 43S preinitiation complex (PIC) then attaches to the mRNA (**Figure 1**) (reviewed in Reference 1). Attachment of the 43S complex is confined to the free 5′ end of the mRNA—indeed, PICs cannot attach to circular mRNAs—and the 5′ untranslated region (5′UTR) is scanned base by base for complementarity to the anticodon (AC) of Met-tRNA$_i$ as successive triplets enter the P site of the 40S subunit. Thus, the first AUG encountered is favored as the start codon, and a novel AUG inserted closer to the 5′ end can become the primary initiation site. Moreover, mutation of the 5′-proximal AUG generally increases initiation from downstream AUGs (2–6).

As first elucidated by Kozak (7), particular sequences immediately surrounding the AUG, especially those including a purine at position −3, enhance AUG selection by the scanning PIC; and a 5′-proximal AUG that deviates sufficiently from the optimum context, which in mammals is 5′-(A/G)NNAUGG-3′, can be bypassed in an event termed leaky scanning. Shortening the 5′UTR beyond ~20 nt also reduces the efficiency of initiation, a finding that can be exploited to produce an N-terminally extended polypeptide (by inefficient initiation at the 5′-proximal AUG) in addition to the shorter, major isoform (by efficient initiation at the downstream AUG) (reviewed in Reference 8). Another defining feature of the scanning mechanism is its impairment by insertion of stable stem-loop (SL) structures in the 5′UTR upstream of the start codon (9, 10).

Other eukaryote-specific features that facilitate the scanning mechanism are the m^{7}G cap at the 5′ end of mRNA and the cap-binding complex eIF4F, which attaches to the

cap to activate mRNA for 43S PIC attachment. eIF4F comprises the cap-binding protein eIF4E, eIF4G, and the RNA helicase eIF4A. eIF4G is a scaffold with binding domains for mRNA, eIF4E, eIF4A, poly(A)-binding protein (PABP), eIF3 (in mammals), and eIF1 and -5 (in budding yeast). The binding domains for eIF4E, PABP, and mRNA in eIF4G enable assembly of a highly stable, circular mRNA–protein complex—the closed-loop structure. Its eIF4A-binding domain enables eIF4G to activate eIF4A allosterically and recruit it to the cap for local unwinding of mRNA, a process that, together with eIF4G interactions with eIF3, eIF5, or eIF1, facilitates 43S attachment at the 5′ end (reviewed in References 1, 8, 11, 12).

Both the unwinding of the secondary structure and the 5′ to 3′ directionality of scanning require energy, which is provided by ATP hydrolyzed by eIF4A or, in some cases, other DEAD-box helicases, including Dhx29 and Ddx3/Ded1. Scanning also requires an open PIC conformation, stabilized by eIF1 and eIF1A, with contributions from eIF5, eIF2, and eIF3. The ternary complex (TC) is tethered to the open PIC in a metastable state that can sample triplets entering the P site for an AUG. The GTP in the TC is hydrolyzed in the scanning complex, stimulated by the GTPase-activating protein (GAP) eIF5 and the 40S subunit. However, completion of the reaction by phosphate (P_i) release, and accommodation of Met-tRNA$_i$ in the P site, requires additional steps triggered by AUG recognition, including eIF1 dissociation from the 40S subunit and conformational rearrangements involving eIF5, -1A, -2β, and -3c. eIF2-GDP dissociates from the PIC, probably in a complex with eIF5, and joining of the large (60S) subunit is catalyzed by eIF5B to produce an 80S initiation complex (IC) that is competent for protein synthesis (reviewed in References 8 and 11).

eIF2-GDP is recycled to eIF2-GTP by the nucleotide exchange factor eIF2B to regenerate the TC for the next round of initiation, a reaction that is inhibited under stress conditions by phosphorylation of eIF2 on Ser-51 of its α-subunit (**Figure 1**). The binding of eIF4G to the mRNA 5′ end is also controlled by eIF4E-binding proteins (4E-BPs) that compete with eIF4G for eIF4E. Although these processes are the principal means of downregulating initiation globally, gene specificity can be achieved by recruitment of regulatory proteins to, for example, 3′UTR sequences that interfere with initiation factors in the PIC at various steps of the process (reviewed in References 13 and 14).

Unlike in bacteria (in which mRNAs are frequently polycistronic), when ribosomes reach a stop codon in eukaryotic cells, they are normally released from the mRNA and cannot efficiently reinitiate at a downstream AUG codon without the involvement of special mechanisms (reviewed in Reference 15). An important exception involves short 5′-proximal (upstream) open reading frames (uORFs), in which some posttermination 40S subunits remain attached to the mRNA and resume scanning. These rescanning subunits gradually acquire TCs, requiring a minimal distance (scanning time) before the downstream AUG is encountered for efficient reinitiation (16). This principle underlies translational control of yeast *GCN4* mRNA (and mammalian *ATF4*/*ATF5* mRNAs) by multiple uORFs; additionally, the scanning distance and time required to recover the TCs are increased under amino acid starvation conditions by eIF2α phosphorylation and the attendant inhibition of eIF2B and reduction in TC concentration. When TCs are abundant in nonstarvation conditions, essentially all rescanning 40S subunits bind TCs before encountering downstream uORFs 3–4, reinitiate at these sites, and then dissociate from the mRNA to leave the *GCN4* ORF untranslated. (Sequence features at uORFs 3–4 impede resumption of scanning by posttermination 40S subunits.) The reduction in TC levels evoked by eIF2α phosphorylation enables some rescanning subunits to acquire TCs only after bypassing uORFs 3–4 and, thus, reinitiate at *GCN4* instead (**Supplemental Figure 1*a***; follow the **Supplemental Material link** from the Annual Reviews home page at **http://www.annualreviews.org**).

Supplemental Material

Supplemental Material

Importantly, mutations in eIF2, eIF2B, or factors involved in $tRNA_i$ biogenesis that reduce TC formation, or in eIFs or 18S rRNAs that reduce the rate of TC binding to 40S subunits, evoke constitutive derepression of *GCN4* translation (the Gcd$^-$ phenotype) (**Supplemental Figure 1*b***)—a powerful in vivo reporter for this step of initiation. Other defects in AUG recognition or scanning block depression of *GCN4* translation and confer the Gcn$^-$

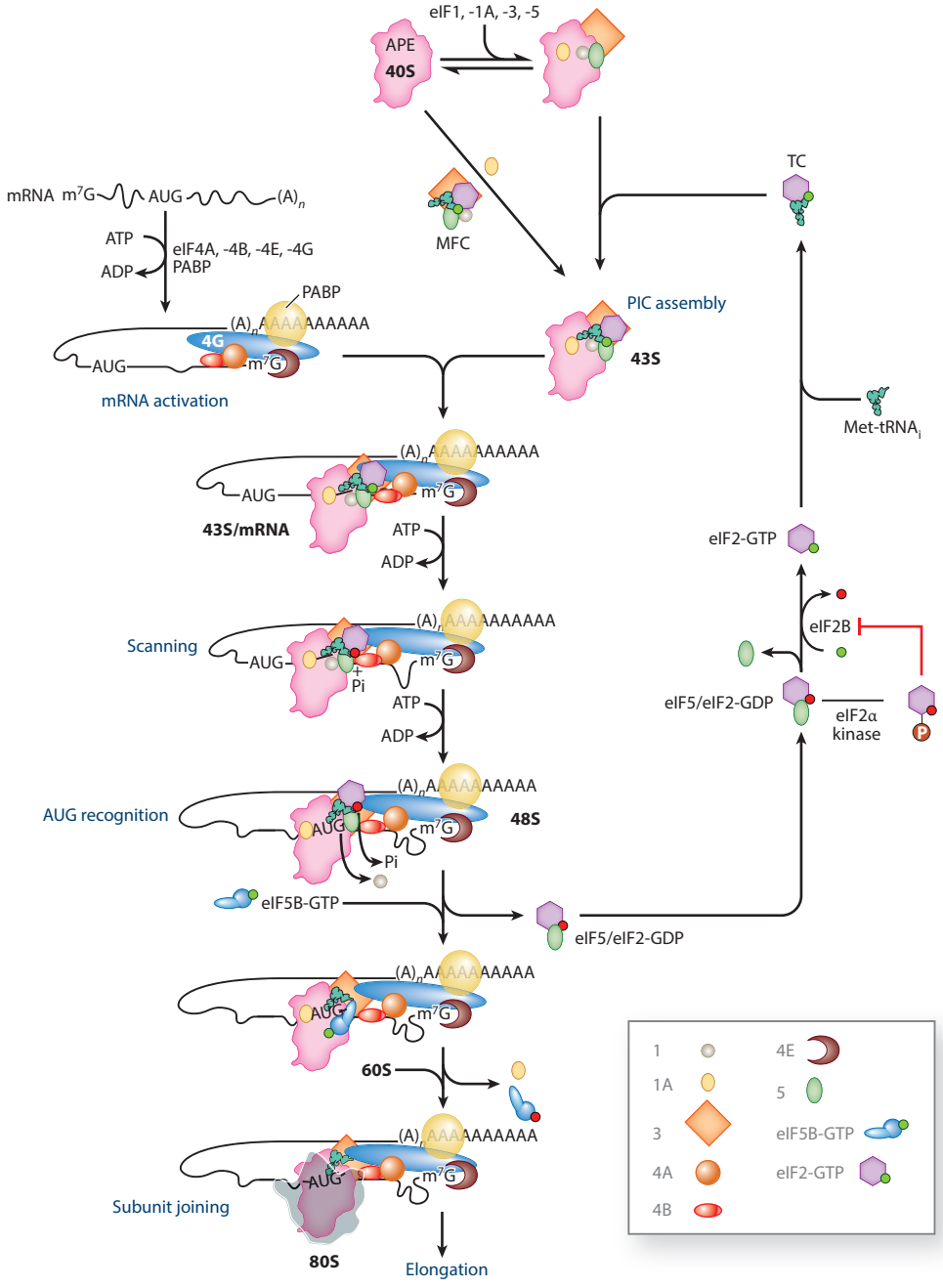

phenotype (**Supplemental Figure 1*c***) (reviewed in Reference 17).

This review focuses almost entirely on initiation via the scanning pathway in budding yeast and mammalian cells. The mechanisms in these eukaryotes are probably similar, but not identical. Although most eIFs display strong sequence similarity between yeast and mammals, this is not the case for eIF4B and eIF4G, and yeast also lacks the eIF4B-related factor eIF4H, helicase Dhx29, and more than half of the 13 subunits of mammalian eIF3 (meIF3) (reviewed in Reference 18). This lesser complexity may reflect, at least in part, the relatively short, unstructured 5′UTRs of most yeast mRNAs (19, 20). Other recent reviews have covered nonscanning mechanisms of initiation via, for example, internal ribosome entry sites (IRESs) (21, 22). Depictions of three-dimensional structures and boundaries of interaction domains for various eIFs can be found in recent reviews on yeast (1) and mammalian (11) translation initiation.

RECRUITMENT OF Met-tRNA$_i$ TO THE 40S RIBOSOMAL SUBUNIT

eIF2-GTP Transfers Met-tRNA$_i$ to the 40S Subunit

Met-tRNA$_i$ is delivered to the 40S subunit in the TC with eIF2-GTP (**Figure 2*a***). The affinity of Met-tRNA$_i$ is ~10-fold greater for eIF2-GTP than for eIF2-GDP, and Met-tRNA$_i$ also increases eIF2 affinity for GTP (23, 24). This thermodynamic coupling depends on the Met moiety (24), and mischarged Ile-tRNA$_i$ binds poorly to eIF2 (25). The first base pair of the tRNA$_i$ acceptor (Acc) stem, A1:U72, enhances Met-tRNA$_i$ binding to eIF2-GTP (24, 26) and, together with contributions from G31:C39 in the anticodon stem loop (ASL) and residues A54 and A60 in the T loop, confers eIF2 specificity for initiator versus elongator Met-tRNA (27, 28) because the latter lacks these conserved signature sequences (29).

Supplemental Material

Although scanning may not occur in archaebacteria, which also lack eIF3, -4, and -5 (30), structural analyses of the archaeal version of eIF2 (aIF2) have provided invaluable information for understanding eIF2 structure and function. Crystal structures of aIF2γ (31, 32) reveal a three-domain protein related to eEF1A (that transfers tRNAs to the A site during elongation) with a GTP binding pocket in the G domain (**Figure 2*a*,*b***). Isolated aIF2γ binds GTP tightly, but strong Met-tRNA$_i$ binding also requires domain III of the α-subunit (aIF2α-III), which interacts with domain II of aIF2γ (aIF2γ-II) (**Figure 2*a*,*b***). However, aIF2β contributes little to binding Met-tRNA$_i$ (33–35). A comparison between structures of free aIF2γ-GDPNP (31) and an aIF2α/aIF2γ-GDPNP heterodimer suggested that binding of aIF2α to aIF2γ opens a channel between the switch 1 (sw1) element in the G domain and aIF2γ-II for the Acc stem of Met-tRNA$_i$ (35), as in the eEF1A TC (36). This prediction is consistent with the structure of an aIF2-GDPNP/fMet-tRNA$_i$ TC, which reveals juxtaposition of the Acc stem and unpaired 3′ residues of tRNA$_i$

Figure 1

Model of a canonical eukaryotic translation initiation pathway. This series of discrete steps begins with assembly of the 43S preinitiation complex (PIC), which is depicted both as a single step via the multifactor complex (MFC) and as two separate steps in which eukaryotic initiation factors (eIFs) eIF1, -1A, and -3 bind to the 40S subunit first, followed by the ternary complex (TC) and eIF5. (The A, P, and E decoding sites are depicted in the 40S subunit.) The 43S PIC is then loaded onto an activated messenger RNA (mRNA)–protein complex near the 5′ cap. Subsequent scanning of the mRNA is accompanied by GTP hydrolysis by the TC without release of phosphate (P_i) from eIF2-GDP. Recognition of the start codon triggers downstream steps in the pathway, including eIF1 dissociation; P_i release from eIF2; and conversion to the closed, scanning-arrested conformation of the PIC. eIF5B in its GTP-bound form promotes joining of the 60S subunit to the PIC, accompanied by release of eIF5B-GDP and eIF1A to form the 80S initiation complex (IC), ready for the elongation phase of protein synthesis. eIF2-GDP, released after subunit joining, is then recycled back to eIF2-GTP by the exchange factor eIF2B; this reaction is impeded by eIF2α phosphorylation. GTP appears as a green ball and GDP as a red ball. Abbreviations: Met-tRNA$_i$, methionyl initiator transfer RNA; PABP, poly(A)-binding protein. Modified from Reference 8 with permission.

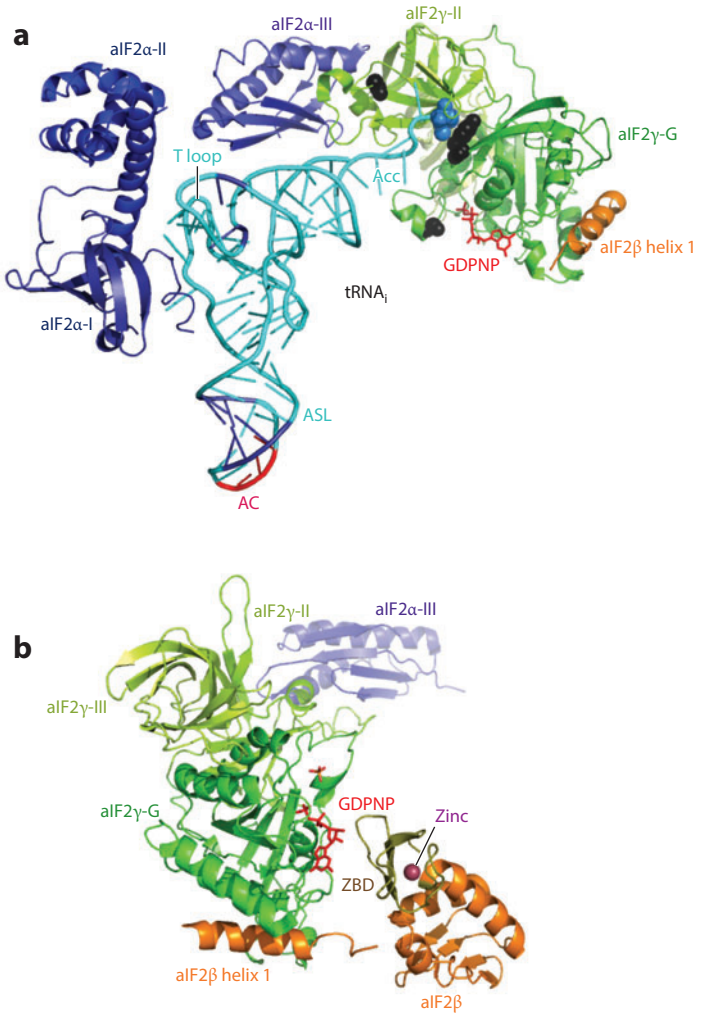

Figure 2

Crystal structures of the *Sulfolobus* archaeal initiation factor 2 (aIF2) and ternary complex (TC). (*a*) Crystal structure of the aIF2-GDPNP/Met-tRNA$_i$ (methionyl initiator transfer RNA) TC. The PyMol image accords with Protein Data Bank (PDB) identifier 3V11 (37). aIF2α-I, amino acids (aa) 1–85 (*deep blue*); aIF2α-II, aa 86–169 (*dark blue*); aIF2α-III, aa 175–264 (*light blue*); aIF2γ-G, aa 7–210 (*green*); aIF2γ-II, aa 211–322 (*chartreuse*); aIF2γ-III, aa 323–415 (*green*); aIF2β helix 1, aa 3–19 (*orange*); *Escherichia coli* tRNA$_i$ (*cyan*); methionine (*blue spheres*). Three signature G:C base pairs in the anticodon stem loop (ASL) and the residues corresponding to T-loop residues A54 and A60 of eukaryotic tRNA$_i$ are colored dark blue, and the anticodon (AC) residues are colored red. Black spheres in aIF2γ-G correspond to residues of which substitutions can reduce Met-tRNA$_i$ binding. (*b*) Crystal structure of aIF2α-III/aIF2γ/aIF2β-GDPNP complex. Image from PDB 2QMU (39). Colors are in panel *a*, except that the aIF2β zinc-binding domain (ZBD) appears in olive.

with sw1 and aIF2γ-II (**Figure 2*a***) (37). It also fits with sw1 mutations of yeast (y)eIF2γ (Y142H, N135K) (23) and β8 of aIF2γ-II (G235D) (34), which impair Met-tRNA$_i$ binding in vitro. Consistently, these yeIF2γ mutations derepress translation of *GCN4* mRNA in vivo (23), a (Gcd$^-$) phenotype indicating reduced TC recruitment to 40S subunits engaged in reinitiation after translation of the first uORF, uORF1, in this specialized transcript (**Supplemental Figure 1*b***) (17). In the archaeal TC structure (37), the Acc stem interacts with aIF2α-III, and the tRNA$_i$ "elbow" contacts domain I of aIF2α (aIF2α-I) and aIF2α-II (**Figure 2*a***). To explain why aIF2α-I and aIF2α-II minimally contribute to Met-tRNA$_i$ binding, investigators proposed that their contributions to the binding energy are offset by decreased entropy in the TC (37), given that these domains are flexible in free aIF2. Indeed, it appears that aIF2 contains a rigid core composed of aIF2γ, aIF2α-III, and the α1-helix of aIF2β (wedged between two helices of aIF2γ-G) (**Figure 2*a***), whereas aIF2α-I, aIF2α-II, and the αβ- and zinc-binding domains (ZBDs) of aIF2β are highly mobile (38–41).

Although mutagenesis of the eukaryotic factor supports an eIF2α/eIF2γ interface (32) similar to that observed in aIF2 (35, 40), eliminating the α-subunit from yeIF2 reduces Met-tRNA$_i$ affinity only slightly (42). Moreover, a model derived from directed hydroxyl radical cleavage (DHRC) mapping of Met-tRNA$_i$ binding to yeIF2 in reconstituted PICs revealed contacts exclusively with eIF2γ that differ dramatically from those observed in the eEF1A TC. Rather than interacting with the tRNA T stem, eIF2γ-III rotates ~180° to interact with helix 44 (h44) of 18S rRNA, providing the key 40S contact of yeIF2 in the PIC (**Figure 3*a***) (43). This functional reassignment of eIF2γ-III was also observed in the archaeal TC structure, accompanied by a kink in the Acc stem that should enable methionylated A76 to occupy the eEF1A like amino acid binding pocket in aIF2γ (37).

Supplemental Material

Despite the lack of evidence for eIF2α/eIF2β contacts with Met-tRNA$_i$ in yeast TCs, each of these yeast subunits dramatically increased the affinity of aIF2γ for Met-tRNA$_i$ in chimeric aIF2/eIF2 complexes (44). Similarly, the α- and β-subunits individually increased the affinity of eIF2γ for Met-tRNA$_i$ in a reconstituted protozoan TC, implicating their overlapping contributions to Met-tRNA$_i$ binding

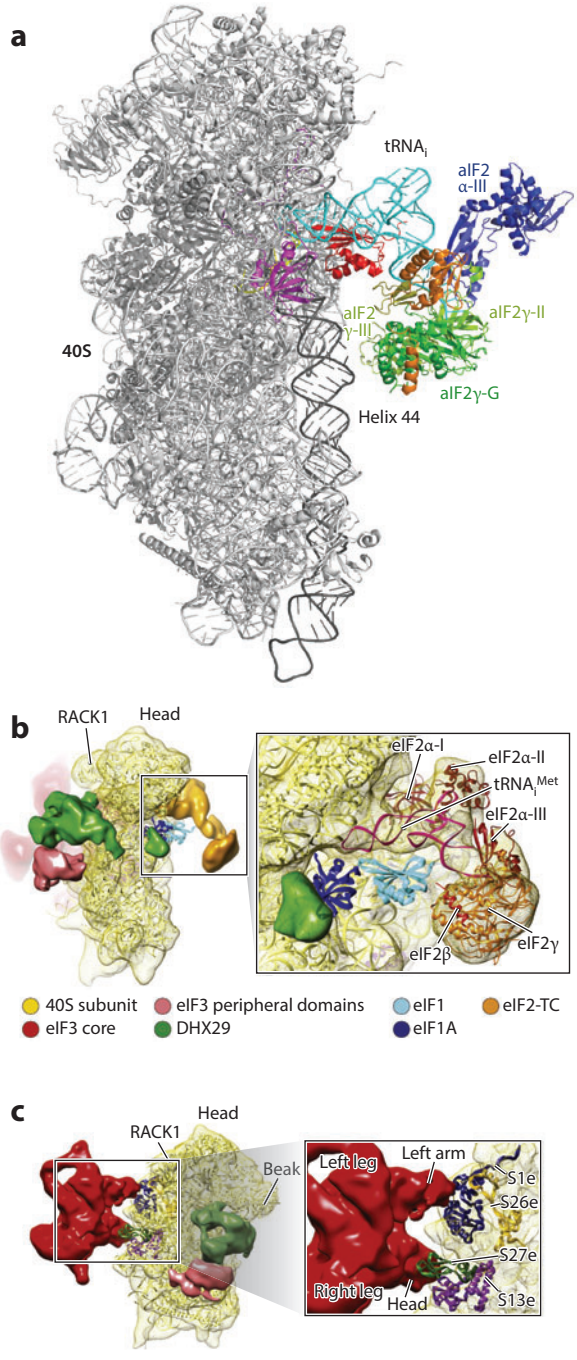

Figure 3

Structural models of the 43S and 48S preinitiation complexes (PICs). (*a*) Modification of the Shin et al. (43) model, rotated so that the 40S subunit interface and decoding sites are on the right. These authors constructed this model with PyMol by docking tRNA$_i$ [Protein Data Bank (PDB) identifier 1YFG] in the P site of the yeast 40S ribosome (PDB 3U5B/3U5C; Stm1 is hidden) in the same location as observed in a bacterial 70S complex (PDB 2J00), by docking aIF2γ (*green*) of the aIF2α/aIF2γ heterodimer (PDB 2AHO) on the acceptor stem of tRNA$_i$ as observed in the bacterial elongation factor Tu (EF-Tu) ternary complex (TC) (PDB 1TTT), and by rotating aIF2γ-III to juxtapose with helix 44 to be consistent with directed hydroxyl radical cleavage data. The NMR structures of human eukaryotic initiation factor 1A (eIF1A) (PDB 1D7Q) (*purple*) and *Tetrahymena* eIF1 (PDB 2XZM) (*red*) were docked on the 40S subunit in the analogous positions observed in the 30S/eIF1 complex (PDB 1HR0) and the 40S/eIF1 complex (PDB 2XZM), respectively. aIF2β (*orange*) was docked onto aIF2γ as observed in the aIF2β/aIF2γ heterodimer (PDB 2QMU), and messenger RNA (mRNA) (*yellow*) was docked on the 40S subunit as observed in a bacterial 70S complex (PDB 2J00). (*b*) Position of the TC in a cryo–electron microscopy (cryo-EM) model of the mammalian 43S/Dhx29 complex. The crystal and NMR structures of eIF1 and eIF1A, respectively, were docked onto the model, and a rigid-body fitting of the crystal structure of archaeal TC on the density assigned to TC is depicted in the close-up. The orientation of the 40S subunit is similar to that in panel *a*. (*c*) Predicted interactions between the left arm and the head of eIF3 (*red*) with ribosomal proteins near the mRNA exit channel in the cryo-EM model of 43S/Dhx29. The *Tetrahymena* 40S crystal structure was fitted as a rigid body into the density assigned to the 40S subunit. The 40S is rotated from the orientation in panel *b* to display the solvent-exposed side of the subunit. Modified with permission from Reference 46.

(45). A recent cryo–electron microscopy (cryo-EM) model of a mammalian 43S PIC containing a TC; eIF1, -1A, and -3; and Dhx29 (46) predicted interactions between (*a*) eIF2α-II and eIF2α-III and (*b*) the Acc and T stems of Met-tRNA$_i$, with eIF2α-II rotated ~45° from its position in the archaeal TC (**Figure 3*b***) (37). In contrast, eIF2α-I does not contact Met-tRNA$_i$ but instead approaches Rps5/S7 near the E site. (For the remainder of this review, at the first mention of a ribosomal protein, the species-specific name is followed by the family name, according to Reference 47.) Because eIF2γ-III is ≥34 Åfrom h44, this eIF2α-I/Rps5 contact is the only interaction between eIF2 and 40S that is visible in the 43S/Dhx29 PIC (**Figure 3*b***) (46). The eIF2α-I/Rps5 contact is consistent with cross-linking of meIF2α to the −3 position of mRNA in reconstituted 48S PICs and the reduced activity of TCs lacking the α-subunit in PIC assembly (48), but it seems inconsistent with the fact that eIF2α is dispensable in yeast when its contribution to eIF2 recycling by eIF2B is compensated genetically (42, 49). Whether the different eIF2/40S contacts observed by DHRC mapping and cryo-EM reflect differences between 40S–TC interactions in yeast versus mammals, or between 43S and 48S PICs, remains to be determined.

Ternary Complex Recruitment Is Enhanced by Other Eukaryotic Initiation Factors That Bind the 40S Subunit and One Another

Studies in reconstituted mammalian and yeast systems showed that eIF1, -1A, and -3 stimulate TC binding to 40S subunits, with generally additive effects (50–59). These factors bind 40S subunits directly (57, 60–64) and, at least for eIF1 and eIF1A, cooperatively (57, 58, 62). The structures of eIF1 and eIF1A have been determined in solution (65–68), and DHRC mapping (69) and crystallography of 40S/eIF1/eIF1A complexes (70, 71) placed the eIF1A oligonucleotide/oligosaccharide-binding (OB) fold in the 40S A site, whereas DHRC mapping (72) and crystallography of 40S/eIF1 and 40S/eIF1/eIF1A complexes (68, 70, 71) placed eIF1 on the 40S platform near the predicted position of the Met-tRNA$_i$ in the P site (**Figures 3*a*** and **4*a***) (68). Investigators have implicated the unstructured N-terminal tail (NTT) of eIF1 (73) and the C-terminal tail (CTT) of eIF1A (74–76) in TC recruitment by identifying Gcd$^-$ substitutions in these segments, which reduced the rate of TC binding to 40S subunits in vitro without impairing 40S binding by the mutant factors themselves. A substitution in the α2-helix of eIF1 (73) and overexpression of a defective C-terminally tagged form of eIF1 likewise conferred Gcd$^-$ phenotypes and reduced the amounts of eIF2 associated with native 40S subunits (77).

eIF3 is a multisubunit complex whose structure is only now beginning to emerge; it differs significantly between yeast and mammals (reviewed in Reference 18). meIF3 consists of 13 subunits (a through m) (61, 78), of which only 6 (a, b, c, g, i, and j) constitute yeIF3 (79, 80). yeIF3b appears to bridge the j/b/g/i and a/c/b subcomplexes (reviewed in References 18 and 81), and although g and i are essential in vivo, in an eIF3 mutant extract the a/c/b subcomplex rescued TC and mRNA recruitment to 40S subunits (82). Mass spectrometry of subcomplexes dissociated from meIF3 (81) and reconstitution experiments support the occurrence of yeastlike subcomplexes in meIF3 (61, 83), although subunits not present in yeast (e, f, and h) were needed, together with the a/b/c trimer, to support 48S PIC assembly in vitro (84). Another reconstitution study confirmed scaffolding functions for subunits a and c but described a distinct stable octamer composed of subunits a, c, e, f, h, k, l, and m (83). Cryo-EM analysis of both this reconstituted octamer (83, 85) and native meIF3 (86) revealed an extended five-lobed "hand," implying that only about half of the mass of meIF3 assumes a rigid core structure. A recent EM analysis of heIF3 complexes assembled with genetically tagged subunits, allowing localization of the N termini of 9 different subunits and comparison between the resulting structure and that of the 19S proteasome lid, led to a structural model for the

meIF3 core wherein 6 PCI domains (common to subunits of the proteasome, COP9 signalosome, and eIF3) interact to form a horseshoe-shaped structure at the base of the complex (85). High-resolution structures are available only for the isolated RNA recognition motif (RRM) of meIF3g (87), a subcomplex of meIF3b RRM and a segment of meIF3j (88), the yeIF3i β-propeller domain bound to the C-terminal helix of yeIF3b (89), and human eIF3k (90).

40S binding by eIF3 is enhanced by its j-subunit (61, 91, 92) and, for meIF3, single-stranded RNA and the TC when meIF3j is missing (58). DHRC mapping placed meIF3j-CTD (C-terminal domain) in the 40S A site, an interaction that seems to impede mRNA binding prior to TC recruitment (93). meIF3j is less tightly associated with the PIC after mRNA binding (78), but it probably remains attached (93) and may function during scanning (88). A cryo-EM analysis suggested that meIF3 binds primarily to the solvent-exposed "backside" of the 40S near the mRNA exit channel (86), in accordance with cross-linking of meIF3a and meIF3d to mRNA at position −14 in reconstituted mammalian PICs (94).

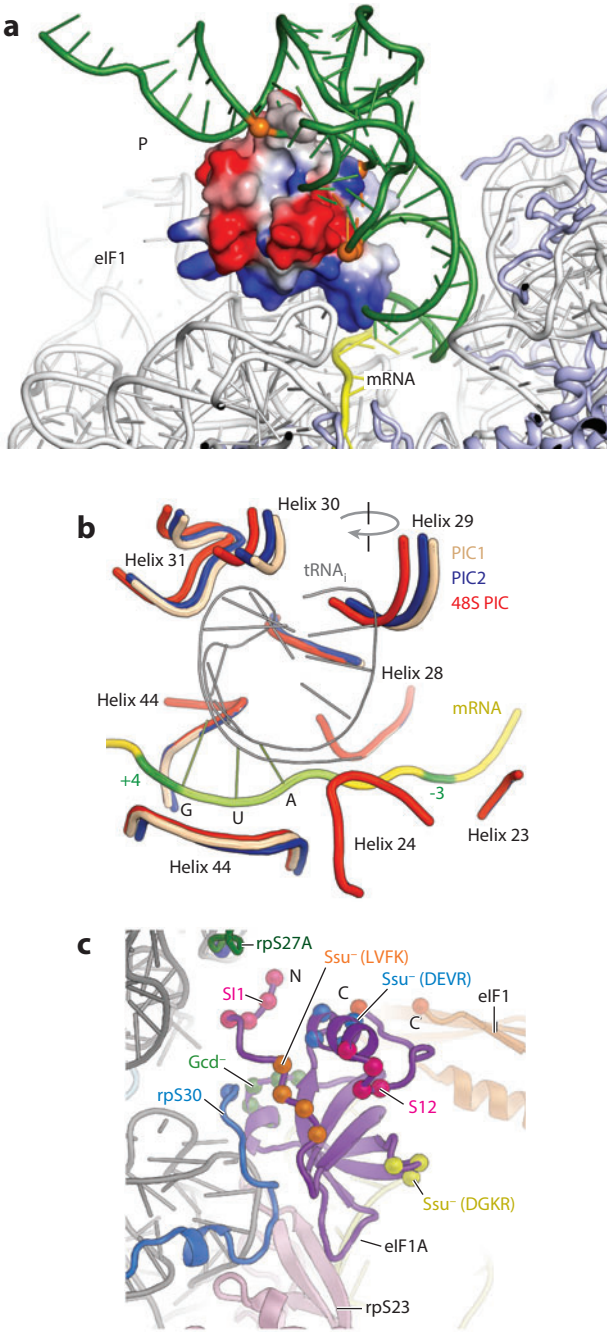

Figure 4

Eukaryotic initiation factor 1 (eIF1), P-site elements, and the eIF1A N-terminal tail (NTT) control the orientation of methionyl initiator transfer RNA (Met-tRNA$_i$) binding in the preinitiation complex (PIC). (*a*) Messenger RNA (mRNA) (*yellow*) and P-site tRNA (*green*) modeled into the *Tetrahymena* 40S/eIF1 crystal structure to depict the predicted clash of eIF1 with the anticodon stem loop (ASL) of Met-tRNA$_i$ bound in the canonical P/P state. (*b*) A superposition of 18S ribosomal RNA helices in the P site in the crystal structures of mammalian 40S/eIF1 (PIC1, *pink*), 40S/eIF1/eIF1A (PIC2, *blue*), and 40S/mRNA/tRNA$_i$/eIF1A (48S PIC, *red*), illustrating how Met-tRNA$_i$ theoretically tilts toward the E site in PIC2 during the scanning process. (*c*) eIF1A in the *Tetrahymena* 40S/eIF1/eIF1A crystal structure, illustrating how different segments of the eIF1A NTT bridge the head and body of the 40S subunit by interacting with Rps27A/S27e and Rps30/S30e. The location of scanning inhibitor 1 (SI1) in the unstructured NTT is indicated. Also depicted is SI2, encompassing residues in the helical domain and its associated structured N and C strands, the locations of particular Ssu⁻ mutations that suppress aberrant UUG initiation in Sui⁻ mutants, and a Gcd⁻ substitution (75, 76). Panels *a*, *b*, and *c* modified from References 68, 70, and 71, respectively.

Consistent with this finding, yeIF3a-NTD (N-terminal domain) interacts with yeast Rps0/S2 (68, 95) in a manner that promotes 40S binding of yeIF3 (96, 97). Enzymatic footprinting and hydroxyl radical cleavage suggested that meIF3 also contacts h16 near the mRNA entry channel (94), and yeIF3a-CTD interacts with h16/h18 (96), Rps2/S5, and Rps3/S3 (98)—all situated near the entry channel (47). These and other findings (87, 88, 99) suggest that eIF3 spans the entry and exit channels on the backside of the 40S subunit. In support of this hypothesis, a cryo-EM model of the 43S/Dhx29 PIC posits that the head and left arm of the meIF3 handlike structure contact Rps13/S15-NTD and Rps27/S27e, and that the left arm contacts Rps3A/S1e and Rps26/S26e, near the 40S exit channel; the additional density is attributed to eIF3 located near Dhx29 at the entry channel (**Figure 3*c***) (46). No meIF3 connections have been observed with Rps0A/S2, Rps2, or Rps3, which (as just mentioned above) are implicated in yeIF3 contacts with the 40S subunit, nor was meIF3 density observed near the predicted binding sites for eIF1 (68), eIF5-CTD (100), or eIF2 on the interface side of the 40S. However, because much of meIF3 is flexible, it may communicate dynamically with factors bound to the interface side of the 40S subunit (83), which would accord with A-site binding of meIF3j-CTD (93) and interactions between yeIF3 subunits and eIF1, -2, and -5 in the multifactor complex (MFC) that promote 40S binding of eIF3, TC recruitment, or AUG recognition in yeast cells (96, 101, 102).

The yeast MFC is stabilized by (*a*) eIF5-CTD interactions with eIF2β-NTT, eIF3c-NTD, and eIF1; (*b*) eIF1 interactions with eIF2β-NTT and eIF3c-NTD; and (*c*) eIF3a-CTD interactions with eIF2β (77, 79, 101, 103–105). There is evidence that the eIF5-CTD/eIF2β-NTT interaction promotes eIF5-CTD binding to the eIF3c-NTD and that the resulting trimeric complex nucleates yeast MFC assembly (105). Various genetic, biochemical, and structural analyses have been used to map (*a*) interactions among eIF1 (67, 100), eIF5-CTD (100, 106), eIF3c-NTD (102, 107), and eIF3a-CTD (101) and (*b*) interactions between each of those segments and eIF2β-NTT (100, 103, 108). Mutations in the eIF5 or eIF3a segments that disrupt these connections impair cell growth in a manner mitigated by TC overexpression (101, 103–105, 109). Gcd$^-$ phenotypes and reduced 40S occupancy of eIF2 have also been identified for substitutions in eIF5-CTD that weaken its binding to eIF2β-NTT (106). eIF3c-NTD mutations probably reduce TC recruitment by weakening the interaction between eIF3c-NTD and eIF5-CTD or the ability of eIF5-CTD to interact with eIF2β-NTT in the MFC (107). These findings, and the fact that depleting any one MFC component reduces the 40S occupancies of all the others in yeast cells (110), support a role for the MFC in efficient PIC assembly in vivo (**Figure 1**). With some differences in relative affinities, interactions that stabilize the yeast MFC have been demonstrated for the mammalian factors (63, 65, 100, 108, 111, 112), and the mammalian MFC appears to be the primary reservoir of eIF3 in mammalian cells. Although the stimulatory effect of mammalian MFC components on TC recruitment can occur without the preassembly of these components prior to 40S binding in vitro (63), it seems likely that the preformed MFC provides a major pathway to TC recruitment in vivo.

43S PREINITIATION COMPLEX ATTACHMENT TO mRNA

eIF4G Activates eIF4A and Recruits the 43S Preinitiation Complex to mRNA 5′ Ends

Preferential selection of 5′-proximal AUGs depends on the fact that 43S PICs attach to mRNA and initiate scanning near the m^{7}G cap. eIF4F is central to this process because eIF4E binding to the cap recruits eIF4G/eIF4A to the 5′ end (reviewed in Reference 11). eIF4G increases eIF4A's ability to stimulate translation (113–117), presumably by recruiting eIF4A and activating its

ATP-dependent RNA helicase activity (118, 119). Interaction with the HEAT domains of eIF4G juxtaposes the RecA-like domains of eIF4A with determinants for RNA binding and ATP binding/hydrolysis poised at the interface (119–122). Recent research suggests that eIF4E stimulates eIF4A helicase activity by its interaction with eIF4G, which appears to overcome an autoinhibitory activity in eIF4G (123). Activation of eIF4A should generate single-stranded RNA near the cap; indeed, mRNAs with more-structured 5′UTRs display a greater requirement for eIF4A and eIF4F in 43S recruitment (124–127). Whereas 43S attachment to unstructured mRNAs can occur in reconstituted systems without eIF4F or ATP (126, 127), eIF4A promotes translation of mRNAs even with short 5′UTRs lacking obvious structure (125, 128). Consistently, mRNAs whose translation was reduced the most in yeast cells depleted of eIF4G had, on average, short 5′UTRs (129). Thus, RNA–RNA interactions, in addition to stable SLs, probably impede 43S attachment to natural mRNAs in a manner mitigated by eIF4F. Similar to other DEAD-box helicases, eIF4A is not a processive enzyme and it is thought to disrupt short helices in mRNA (130) and bind to the resulting unpaired strands, and is then released from the mRNA on ATP hydrolysis for subsequent rounds of melting (131; reviewed in Reference 132). Evidence suggests that the half-open conformation of the RecA-like domains evident in the yeIF4A/eIF4G-HEAT crystal structure (119) facilitates P_i release following ATP hydrolysis (122).

In addition to recruiting and activating eIF4A, meIF4G apparently helps recruit the 43S PIC directly by interacting with eIF3e (133, 134). Neither eIF3e nor the eIF3-binding segment of meIF4G is present in yeast (135), and yeIF3 and yeIF4G seem not to directly interact (127, 136). However, yeIF4G interacts with eIF5 (127), and eIF5-CTD can bridge yeIF4G2 interaction with eIF3c-NTD and can stimulate eIF4G/eIF3 association in yeast extracts (136). Given that eIF5 can bind directly to 40S subunits (64), it may also bridge eIF4G/40S association; indeed, eIF5-CTD mutations that reduce their interaction with eIF4G2 impair 43S binding to mRNA in yeast extracts (136). Because a stimulatory function of eIF5 in mRNA recruitment was not observed in the reconstituted yeast system (127), the interaction between eIF5 and eIF4G may be redundant with other interactions that enhance 43S attachment to mRNA.

Multiple Interactions Stabilize eIF4G/mRNA Association in the Closed-Loop Intermediate

Simultaneous binding of eIF4E to the cap, PABP to the poly(A) tail, and eIF4E and PABP to their binding sites in eIF4G-NTD enables circularization of the mRNA (**Figure 1**) (reviewed in Reference 11). Although it is frequently assumed that this closed-loop conformation is crucial for PIC recruitment, the importance of the interaction between PABP and eIF4G varies with cell type. Elimination of the PABP-binding domain in yeIF4G impairs the stimulatory effect of the poly(A) tail on translation in yeast extracts but has little effect on cell growth unless both (*a*) the interaction between eIF4G and eIF4E is impaired (137) and (*b*) the RNA-binding region in the N terminus of yeIF4G1 (RNA1) is removed (138). Thus, RNA1 and the PABP/eIF4E-binding domains in yeIF4G collaborate to stabilize the binding of eIF4G to mRNA near the cap, and the closed loop may be incidental to efficient 43S attachment. Impairing the interaction between PABP and meIF4G also had a modest effect on translation in rabbit reticulocyte lysates (139), but it substantially impaired eIF4E binding to the cap, 48S assembly, and 60S subunit joining in Krebs-2 extracts (140). Considering that addition of the RNA-binding protein YB-1 to rabbit reticulocyte lysates confers PABP dependence (141), interaction between PABP and eIF4G may be critical only when RNA-binding proteins are available to effectively compete with eIF4G for direct binding to mRNA (142). The increased probability of 5′- and 3′-end

association and PABP–eIF4G interaction afforded by shorter mRNAs may help explain the inverse correlation between the length of coding sequences and translational efficiency (143). Although the eIF4E–cap interaction adds little to the binding affinity of eIF4F for mRNA in vitro (144), it should enhance competition by eIF4F with general RNA-binding proteins and is important for positioning eIF4F at the 5′ end.

yeIF4G1 contains RNA-binding domains in its middle region and at its C terminus (RNA2 and RNA3, respectively) that appear to be functionally redundant (145) and to act downstream of eIF4F/mRNA/PABP assembly (138). Multiple Arg residues in the RNA2 region of yeIF4G2 seem to promote 43S/mRNA attachment, at least partly by promoting interaction between RNA2 and eIF5 (146). The RNA2 and RNA3 domains in yeIF4G1 impart directionality to RNA duplex unwinding by eIF4F, enhancing unwinding for substrates with single-stranded 5′ overhangs while impeding the reaction for substrates with 3′ overhangs (147). RNA3 also contains a binding site for Ded1 (148), an essential yeast helicase that has been implicated in scanning (149, 150; reviewed in Reference 8). Although eliminating the eIF4G-binding domain in the C terminus of Ded1 impairs translation in vitro, it does not affect cell growth (148); these findings suggest that Ded1 can be recruited by a redundant pathway in vivo.

eIF4B Enhances 43S/mRNA Assembly by Multiple Mechanisms

The helicase activity of meIF4A is stimulated by the related proteins eIF4B and eIF4H (118, 151). Consistent with this finding, introduction of a G+C-rich sequence into the globin mRNA 5′UTR increases the requirement for eIF4B in 48S PIC assembly in vitro (152), and depletion of eIF4B from mammalian cells seems to preferentially reduce translation of mRNAs with more structured 5′UTRs (153). How meIF4B stimulates eIF4A helicase function is unclear. It may enhance binding of ATP and RNA by eIF4A (135, 151, 154, 155) and increase the efficiency of coupling ATP hydrolysis to duplex unwinding by eIF4F (156). For the latter activity, eIF4H is less effective than meIF4B (156), consistent with its inability to replace meIF4B in promoting 48S PIC assembly on an mRNA with structured 5′UTR. The inability to replace meIF4B might reflect the absence in eIF4H of the C-terminal RNA-binding region found in meIF4B, which is instrumental in stimulating eIF4A helicase activity (151). eIF4B's single-stranded RNA–binding activity might also enable it to recruit eIF4A to duplex-containing substrates with single-stranded overhangs (151) or to capture single-stranded products and prevent reannealing.

Investigators previously found that yeIF4B (Tif3) does not stimulate yeIF4A helicase activity in vitro (147, 157), even though yeIF4A can be activated by meIF4B (124) and meIF4B can functionally replace yeIF4B in a yeast extract (158). Nevertheless, yeIF4B was required along with eIF4F and eIF3 in the reconstituted yeast system for rapid 48S PIC assembly on native mRNAs with short 5′UTRs (127), where it reduces the concentration of eIF4A required for 43S/mRNA attachment (160). A recent study reported that yeIF4B can function similar to meIF4B to increase coupling between ATP hydrolysis and duplex unwinding by eIF4A/eIF4G complexes, presumably by lengthening the dwell time of the closed conformation of eIF4A to allow sufficient time for RNA strand displacement prior to ATP hydrolysis (161). In vivo, yeIF4B also promotes association between eIF4G and eIF4A (162). Interestingly, yeIF4B binds directly to the 40S subunit and interacts with Rps20/S10, exposed on the backside of the 40S, and protects rRNA residues from chemical cleavage near the mRNA entry channel. Thus, yeIF4B may facilitate 43S/mRNA interaction by modulating the entry channel latch in addition to promoting eIF4A function (160). Elimination of yeIF4B greatly reduces cell growth (especially at low temperatures) and bulk mRNA translation (159), and the absence of yeIF4B also decreases native 43S attachment to mRNAs with short 5′UTRs (160). Given that the effect of deleting *TIF3* on reporter translation was exacerbated

by an SL insertion near the cap (158), in vivo yeIF4B apparently acts broadly to promote 43S PIC attachment but is particularly important for mRNAs with structured 5′UTRs.

meIF4B binds in vitro to eIF3a through internal DRYG repeats, which lack eIF4H, and may form a protein bridge between the eIF4F/mRNA protein and PIC, acting redundantly with the interaction between eIF3 and eIF4G (163). Also, meIF4B may stimulate 43S attachment more directly by binding to mRNA through its C-terminal RNA-binding domain, and 18S rRNA via its RRM (164). Although these are viable possibilities for meIF4B, the RRM in yeIF4B (and the single-stranded RNA–binding activity it confers) is largely dispensable for stimulating 48S PIC assembly in vitro and bulk translation in vivo. Instead, an internal domain of ~26–amino acid repeats, not evident in meIF4B, is the critical segment in yeIF4B, with an auxiliary contribution from the NTD (160).

eIF3 Stimulates 43S Preinitiation Complex Attachment to mRNA

eIF3 from mammals (50, 51) and yeast (82, 110, 127) promotes 43S PIC binding to native mRNAs and, consistently with a direct role in this process, more strongly stimulates 48S than 43S formation (50, 51, 56, 127). Moreover, binding of meIF3 to 40S subunits is stimulated by single-stranded RNA (58, 78), and meIF3a and meIF3d can be cross-linked to mRNA residues in the exit channel of 48S PICs (94). Consistent with these findings, yeIF3 more strongly enhances 43S binding to mRNA harboring a long 5′UTR (which would protrude from the exit channel) than to mRNA containing a short leader (127). However, because yeIF3a-CTD has been implicated in 43S attachment and appears to reside near the mRNA entry channel (98), eIF3 may also interact with mRNA at this location. As mentioned above, a cryo-EM model of the 43S/Dhx29 complex implicates meIF3/40S contacts in the vicinity of both the exit and entry channels of the mRNA-binding cleft (46).

SCANNING AND AUG RECOGNITION

The 43S PIC scans the 5′UTR by using the AC of Met-tRNA$_i$ to identify the AUG codon. Scanning apparently depends on both a 40S conformation conducive to processive movement along the mRNA and the unwinding of duplex structures to enable the mRNA to thread through the 40S/mRNA-binding cleft and expose successive triplets in the P site. Measurements of the effect of 5′UTR length on the time required for the first round of translation indicated that scanning occurs at ~8 bases/s and that it exhibits a strong bias toward 5′ to 3′ movement (149, 165). Some evidence shows that this process involves a series of forward, 5′ to 3′ steps punctuated by limited backward, 3′ to 5′ excursions (166). That increasing 5′UTR length did not reduce translational efficiency in yeast cells implies that multiple PICs can simultaneously scan the same 5′UTR (149).

Functions of RNA Helicases in Scanning

DEAD-box RNA helicases have been implicated in facilitating scanning through long or structured 5′UTRs. eIF4A, together with eIF4F, eIF4B, and ATP, was required for 48S assembly in the mammalian reconstituted system when an SL was placed in an unstructured 5′UTR at a location (43 nt from the cap) where it should not impede 43S attachment (126). This finding indicates that ATP hydrolysis by eIF4A stimulates scanning through SLs. Consistent with a role for eIF4G in scanning, a segment of meIF4G N-terminal to HEAT-1, with RNA-binding activity, was required for scanning subsequent to 43S attachment to certain viral IRESs (167). The finding that eIF4G2 substitutions that weaken its binding to eIF4E or eIF4A appear to reduce the rate of scanning by reinitiating PICs on *GCN4* mRNA (168) may indicate that eIF4G promotes scanning as a component of eIF4F while still bound to the cap structure.

The locations of the eIF4 factors in the scanning complex are unclear. On the basis of (*a*) early findings that mRNA nucleotides positioned 5′ of the 40S subunit in mammalian 43S-mRNA complexes are protected from RNase digestion (169, 170) and (*b*) a cryo-EM reconstruction (86), eIF4G may be positioned at the mRNA exit channel of the 40S subunit and may act to pull mRNA through the 40S subunit. Other investigators have suggested that eIF4G delivers eIF4B/eIF4A-ATP complexes to single-stranded mRNA emerging from the exit channel to prevent backsliding until the PIC moves forward again (171). Re-forming duplex structures as the mRNA emerges may also prevent backward motion, and eIF4B possesses reannealing activity (157, 172); however, the dispensability of the eIF4B RRM domain in yeast (160) suggests that this activity either is unimportant or can be supplied by another factor. Yet another proposal is that eIF4G spans the exit and entry channels and positions eIF4A and eIF4B at the entry channel for unwinding duplex structures ahead of the ribosome (135). If so, the RNase protection results cited above imply that the proposed interactions between eIF4A/eIF4B and mRNA downstream of the scanning PIC are transient.

Whereas eIF4F, eIF4A, and eIF4B function poorly in the mammalian system to stimulate scanning through strong SLs of −19 kcal/mol or less, helicases Dhx29 and yDed1 can do so (150, 173). Interestingly, Dhx29 and Ded1 cannot take the place of eIF4F for 48S PIC assembly on β-globin mRNA, suggesting that Dhx29 and Ded1 specifically stimulate scanning through secondary structures and that eIF4F enhances both 43S attachment and scanning but is relatively less effective at resolving strong SLs (150). Protection of 18S rRNA in the 40S subunit from chemical modification by Dhx29 (173) and cryo-EM analysis of the 43S/Dhx29 complex (**Figure 3*c***) (46) place Dhx29 at the mRNA entry channel. Because it is not a processive helicase and its ATPase activity is stimulated by the 43S PIC, Dhx29 may act by stimulating opening of the entry channel to capture single-stranded bases melted from the SL. A double-stranded RNA–binding motif in the Dhx29 NTD is critical for its binding to the 43S PIC, and both an insert in the second RecA-like domain and a C-terminal OB fold couple ATPase activity to 43S and RNA binding by Dhx29, as well as promote scanning through SLs (174). Considering the significant reduction in protein synthesis evoked by Dhx29 knockdown in mammalian cells (175), Dhx29 might also enhance translation of many mRNAs lacking strong SLs.

Ded1 is likewise required for translation of most yeast mRNAs (176), and genetic data suggest that it functionally overlaps with eIF4F, eIF4B (177), and helicase Dbp1 in vivo (178). Interestingly, a *ded1* mutation or a *DBP1* deletion had stronger effects than did an eIF4A mutation or a *TIF3* deletion on the translation of a reporter harboring a long 5′UTR (149). This observation suggests that Ded1 and Dbp1 are more important than eIF4A and eIF4B for processive scanning. Indeed, Ded1 was more potent than eIF4A and eIF4B in unwinding RNA duplexes in vitro (albeit in the absence of eIF4G) (179), and a *ded1* mutation impaired scanning through an SL located distal from the 5′ cap in vivo (98).

Although depletion of the Ded1 homolog, Ddx3, in mammalian cells did not affect global translation, it reduced expression of certain reporter mRNAs with structured 5′UTRs (180). Interestingly, translation of reporters with cap-proximal SLs was rescued in Ddx3-depleted cells by moving the SL further from the cap. Considering that (*a*) displacement of the SL by only 15 nt bypasses Ddx3, (*b*) inhibition of eIF4A with hippuristanol impairs translation of constructs lacking cap-proximal SLs, and (*c*) Ddx3 interacts with eIF4F, it seems likely that Ddx3 is needed to expose an unstructured binding site for eIF4F at the cap, which then promotes PIC attachment (181). Ddx3 also interacts with eIF3 and the 40S subunit (182, 183) and seems to promote joining of the 60S subunit independently of its helicase activity (183). It is difficult to reconcile discrepancies from different knockdown studies about whether Ddx3 is required generally for translation or

only for certain mRNAs harboring particular 5′UTR structures, which might have to do with the extent of knockdown or activities of other helicases present in the cells. Also unclear is whether Ddx3 and Ded1 perform analogous functions in mammals and yeast, respectively.

AUG Recognition by the Scanning Preinitiation Complex

A critical aspect of the scanning process is the ability of the 43S PIC to bypass AUGs in poor surrounding sequence context, as well as near-cognate triplets (those with single-base mismatches from AUG) in the 5′UTR, so that the initiation complex can be assembled at the correct AUG start codon on the mRNA.

Base-pairing of Met-tRNA$_i$ with AUG stabilizes ternary complex binding to the preinitiation complex. Yeast genetic experiments established that base-pairing of the Met-tRNA$_i$ AC with AUG directs start-codon selection in vivo (184), and studies of mammalian PICs reconstituted with AUG triplets (versus mRNA) revealed that base-pairing between AUG and Met-tRNA$_i$ stabilizes TC binding to the 40S subunit (52, 55, 58). In yeast PICs reconstituted with unstructured mRNA, all single-base substitutions at the second or third position of the AUG triplet reduce TC affinity for 43S/mRNA complexes by 10–50-fold, mostly by decreasing the on rate. This reduction in affinity was attributed to a slower conformational change to a more stable complex than what occurs with AUG, UUG, or GUG start codons following the initial encounter of TC with the PIC. The near cognates UUG and GUG still increase the off rate, however, so they elevate the dissociation constant (K_d) 5–10-fold above that for AUG. The range of K_d values roughly parallels the expression of reporter mRNAs harboring different start codons in yeast cells, albeit with notable exceptions, suggesting that the stability of the codon/AC duplex is a key determinant of initiation efficiency (185). The conformational rearrangement posited in this study probably corresponds to the switch from open to closed PIC conformations, which increases the stability of TC binding to reconstituted 43S/mRNA complexes on AUG recognition (186). Evidence shows that *N*6-threonylcarbamoyl modification of A37, adjacent to the AC triplet, also promotes efficient AUG recognition in yeast (187–191).

P-site residues implicated in stable ternary complex binding to the preinitiation complex. The crystal structure of a mammalian complex containing the 40S subunit, nonacylated tRNA$_i$, mRNA, and eIF1A provides a model of the 48S PIC following dissociation of eIF2-GDP (70). In addition to base-pairing with AUG, the ASL interacts with multiple 18S rRNA helices that constitute the P site, similarly to P-site tRNA in bacterial 70S ribosomes (192, 193), except that the tRNA$_i$ is tilted toward the E site [reminiscent of the P/I state of bacterial 30S ICs (194)]. A genetic analysis of yeast 18S rRNA established the involvement of residues in h28 and h44 in stable Met-tRNA$_i$ binding to PICs in vivo by identifying substitutions that conferred dominant Gcd$^-$ phenotypes, recessive lethality, or leaky scanning of *GCN4* uORF1, as well as (for A1152U) a reduced rate and stability of TC binding in vitro (195). A substitution in the h31 loop (A1193U) also impaired start-codon recognition in vivo and reduced Met-tRNA$_i$ binding to 40S subunits in extracts (196).

In bacterial 70S complexes, 16S rRNA residues G1338 and A1339 in h29 make so-called A-minor interactions with base pairs in the ASL (192, 193); these correspond to the first and second of three invariant G:C base pairs that are unique to tRNA$_i$ (29) and appear to stabilize Met-tRNA$_i$ binding to the 30S subunit and promote rejection of elongator tRNAs (197) and near-cognate start codons (198, 199). Consistent with A-minor interactions by the cognate residues in 18S rRNA (G1575 and A1576), substitution of the first and third ASL G:C base pairs in tRNA$_i$ eliminated the stabilizing effect of AUG on TC binding to reconstituted yeast PICs (27), impaired

translation in mammalian extracts (200), and destabilized mammalian PICs following GTP hydrolysis in the TC (201). Moreover, most substitutions of yeast 18S residues G1575 and A1576 are lethal and produce dominant Gcd$^-$ phenotypes and increased leaky scanning of *GCN4* uORF1, indicating PIC instability or impaired AUG recognition (195). However, because substitution of the ASL G:C base pairs in $tRNA_i$ has little effect on yeast growth (202), if the A-minor interactions are crucial for initiation in yeast, there must be flexibility in the allowed "receptor" ASL base pairs (203).

The signature A1:U72 base pair in the Acc stem of $tRNA_i$ enhances TC binding to reconstituted yeast PICs, whereas the conserved T-loop residues A54 and A60 seem to impede Met-$tRNA_i$ binding, given that substitutions here compensate for the deleterious effect of altering the third ASL G:C base pair (27). Considering that A54, A60, and m^1A58 (bearing the *N*1-methyladenosine modification) participate in multiple tertiary interactions (204), the ensuing rigidity may oppose the deformation of Met-$tRNA_i$ required for its stable binding to the P site in the closed PIC conformation, and the energy penalty is provided by the perfect AUG/AC duplex (27, 205).

eIF1, eIF1A, and eIF5 mediate conformational changes that control AUG recognition. Toe-printing experiments indicated that eIF1 and eIF1A are dispensable for attachment of mammalian 43S PICs near the 5′ end of globin mRNA in the presence of eIF4F but that they are necessary afterward to form a 48S complex at the AUG (206). eIF1 is also needed to block recognition of near-cognate triplets and AUGs in suboptimal context, or AUGs located too close (4 nt) to the cap. eIF1/eIF1A may stabilize an open conformation of the PIC that is conducive to scanning, and eIF1 may impede formation of a closed complex until an AUG in good context enters the P site (126). This model agrees with genetic findings that yeIF1 mutations increase initiation from near cognates in vivo—the Sui$^-$ phenotype (207). Subsequently, investigators found that yeIF1 dissociates from the PIC on AUG recognition (59) and that this event is accompanied by release of P_i from eIF2 in the TC of reconstituted PICs. GTP hydrolysis by TCs occurs nearly as quickly before and after AUG recognition, but P_i is released rapidly only after eIF1 is ejected at AUG (208). The critical role of eIF1 in gated P_i release is highlighted by the finding that yeIF1 mutations that slow down or speed up eIF1 dissociation correspondingly alter the rate of P_i release, which occurs at the same rate as eIF1 dissociation (73, 208, 209). Moreover, eIF1 Sui$^-$ mutations generally weaken its binding to 40S subunits and accelerate release of eIF1 and P_i from reconstituted PICs, whereas a substitution in eIF1A-NTT that suppresses UUG initiation [suppression of Sui$^-$ (Ssu$^-$) phenotype] retards eIF1 dissociation in vitro (73). Overexpression of wild-type eIF1 consistently suppresses UUG initiation in Sui$^-$ mutants (76, 102, 210). Presumably, P_i release at UUG codons is not instantaneous, so faster rebinding of eIF1 to the 40S afforded by its overexpression blocks P_i release and allows continued scanning.

A cryo-EM analysis revealed that eIF1 and eIF1A provoke a structural rearrangement of the yeast 40S subunit that involves an open conformation of the "latch" on the mRNA entry channel, which was proposed to be conducive to scanning. By contrast, the 40S/eIF1A complex, which would resemble the PIC following eIF1 release at AUG, displays a closed-latch conformation that was considered incompatible with scanning. Importantly, eIF1 and eIF1A stimulate the rate of TC binding to the 40S, but the TC is bound more tightly in the absence of eIF1 (186). This finding (as well as others regarding eIF1A, discussed below in this section) led to the proposal that the TC binds to the open conformation of the PIC in a metastable state in which the Met-$tRNA_i$ is not fully engaged with the P site (P_{OUT} state), a state that is conducive for scanning but incompatible with start-codon recognition. Base-pairing with AUG stabilizes TC binding with the ASL inserted deep in the P site (P_{IN} state) through an isomerization reaction that

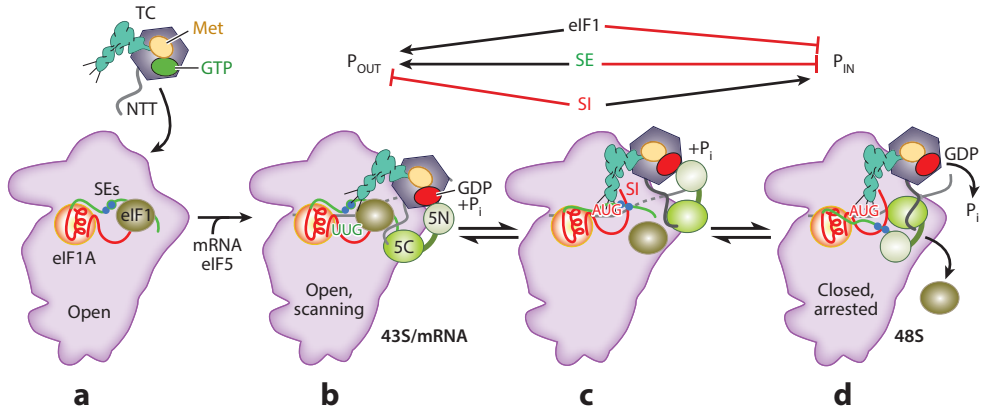

Figure 5

Model of structural rearrangements in the preinitiation complex (PIC) accompanying start-codon recognition. (*a*) Binding of eukaryotic initiation factors (eIFs) eIF1 and eIF1A to the 40S subunit evokes an open conformation conducive to rapid ternary complex (TC) binding, which forms the 43S PIC. [The N-terminal tail (NTT) of eIF2β is shown as a wavy line attached to the TC.] (*b*) The 43S subunit scans the messenger RNA (mRNA) 5′ untranslated region; the anticodon stem loop (ASL) of methionyl initiator transfer RNA (Met-tRNA$_i$) is not fully engaged with the P site (P_{OUT} state) but can sample triplets for complementarity to the anticodon as they enter the P site. The GAP domain in eIF5-NTD (N-terminal domain, abbreviated 5N) stimulates GTP hydrolysis to produce GDP-P$_i$ (phosphate), but release of P$_i$ is impeded. The unstructured NTT of eIF2β interacts with eIF1 to stabilize this open conformation of the PIC. (*c*) Base-pairing between the ASL and the AUG codon promotes movement of the tRNA from the P_{OUT} state to the P_{IN} state, displacing eIF1 from its location near the P site to a new 40S binding site that overlaps with the eIF5-CTD (C-terminal domain, abbreviated 5C) binding site. This movement of eIF1 eliminates its interaction with eIF2β-NTT, and the latter interacts tightly with eIF5-CTD instead. (*d*) eIF1 dissociates from the 40S subunit to stabilize the closed, scanning-incompatible conformation of the 40S subunit. Ejection of eIF1 allows eIF5-NTD to dissociate from the G domain of eIF2γ and bind to the 40S subunit at a location that overlaps the eIF1 binding site, facilitating a functional interaction with the eIF1A C-terminal tail (CTT) that triggers release of P$_i$ from eIF2-GDP-P$_i$ and blocks reassociation of eIF1 with the 40S subunit.

requires eIF1 dissociation and rearrangement to the closed 40S conformation (**Figure 5**) (69, 76, 185, 186). The scanning PIC may transiently rearrange to the P_{IN} state to inspect each triplet entering the P site but rapidly toggle back to the P_{OUT} state in the absence of perfect complementarity to the AC of Met-tRNA$_i$.

A model of the *Tetrahymena* 40S/eIF1 structure with tRNA docked in the P site suggests that eIF1 clashes significantly with Met-tRNA$_i$ in its canonical P/P orientation (**Figure 4*a***) (68). This hypothesis is consistent with the idea that eIF1 impedes Met-tRNA$_i$ pairing with non-AUG codons. This clash would weaken eIF1 binding to the 40S platform when the P_{IN} state is achieved at an AUG codon and would facilitate eIF1 dissociation. A fluorescence resonance energy transfer (FRET) analysis of fluorescent derivatives of yeIF1 and eIF1A revealed that AUG recognition evokes a rapid conformational change that moves eIF1 and eIF1A-CTT apart, followed by slower eIF1 dissociation from the 40S subunit (59). This finding suggests that eIF1 moves rapidly from the platform to a new location in the PIC, driven by the clash with Met-tRNA$_i$, and eventually dissociates after subsequent rearrangements in the PIC (**Figure 5**) (64).

Unstructured yeIF1A-CTT, similar to eIF1, apparently stabilizes the open PIC conformation and the P_{OUT} state of TC binding and must be neutralized to achieve the closed/P_{IN} state at AUG. Short repeats in yeIF1A-CTT, dubbed scanning enhancer (SE) elements, appear to cooperate with eIF1 to promote the open conformation and accelerate TC loading while impeding rearrangement to the closed complex at non-AUG codons. Thus, SE substitutions confer a Gcd$^-$ phenotype and a reduced rate of TC binding

in vitro, as well as elevated UUG initiation (Sui$^-$ phenotype). That overexpressing eIF1 suppresses the Sui$^-$ phenotype (but not the Gcd$^-$ phenotype) of SE mutations suggests that the SE elements directly promote the P_{OUT} state of TC binding and stabilize the open PIC conformation (76). DHRC mapping indicates that the unstructured CTT reaches into the P site and clashes with the ASL in its canonical P-site location (69), suggesting that, similar to eIF1, CTT SE elements must be displaced to enable isomerization to the P_{IN} state (**Figure 5**).

A mutational analysis of yeIF1A-NTT indicates that it contains a scanning inhibitor (SI) element that antagonizes the SE elements in the CTT to promote rearrangement to the closed/P_{IN} state at AUGs (**Figure 5**). In the reconstituted system, SI mutations destabilize the closed 40S conformation (based on 60S subunit joining assays); slow down eIF1 dissociation; restore rapid TC loading to the open conformation; and cosuppress the Gcd$^-$ and Sui$^-$ phenotypes of mutations in eIF1A-CTT, eIF2β, or eIF5 in vivo (73, 75, 76). meIF1A-NTT appears to reach into the P site, but unlike meIF1A-CTT, its predicted location is compatible with the canonical Met-tRNA$_i$ binding (69) presumed to occur for the P_{IN} state.

Recent crystal structures of mammalian 40S complexes harboring eIF1, eIF1/eIF1A, or eIF1A/mRNA/tRNA$_i$ (48S PIC) support the ideas that tRNA$_i$ is more loosely bound to the P site in the scanning complex in a manner that avoids steric clash with eIF1 and that it becomes locked into the P site following AUG recognition (70). The location of the P-site elements of h29 in the 40S/eIF1 and 40S/eIF1/eIF1A complexes may allow Met-tRNA$_i$ to tilt toward the E site and avoid a clash with eIF1 (**Figure 4*b***), fulfilling the requirements of the postulated P_{OUT} state. Owing to a 3–6° clockwise rotation of the 40S head between these two complexes versus the 48S PIC (with tRNA$_i$ base-paired to AUG), h29 moves 2–4 Åtoward the A site, which (together with h24 elements) should prevent tilting of Met-tRNA$_i$ toward the E site and stabilize a P/I-like state that clashes with eIF1, as predicted for the P_{IN} state. Interestingly, the unstructured CTT of Rps15/S19 and the unstructured NTT of eIF1A appear to interact with the ASL in this 48S complex, consistent with the hypothesis that the latter promotes the P_{IN} state. That h28 is the pivot point for the 40S head rotation is consistent with the finding that Gcd$^-$ substitutions in h28 of yeast 18S rRNA confer leaky scanning and destabilize TC binding to 48S PICs (195). Considering that the cryo-EM structure of the 43S/Dhx29 PIC, which presumably depicts the P_{OUT} state, also reveals that Met-tRNA$_i$ (in the TC) tilts toward the E site (46), the movement of Met-tRNA$_i$ between the P_{OUT} and P_{IN} states may be subtle.

The recent crystal structure of eIF1 and eIF1A bound to the *Tetrahymena* 40S subunit (71) reveals no direct interaction between these two factors, but both contact the top of h44 and eIF1A interacts with residue A1709 in the "flipped-out" conformation that the equivalent residue in bacterial h44 (A1492) assumes when interacting with the codon/AC helix in the A site during elongation. The finding that this orientation of A1709 occurs in the eIF1/40S complex (68) may help explain thermodynamic coupling in eIF1/eIF1A binding to the 40S subunit. The h44 also shifts toward eIF1A, which may underlie the ability of eIF1/eIF1A to accelerate TC binding via the predicted h44 contact with eIF2γ-III (43). Interestingly, eIF1A-NTT residues, including those corresponding to the yeast SI1 element in this segment (76), interact with Rps27A/S31e in the 40S head, whereas those in the structured portion of the N strand that belong to a second SI element (SI2) interact with the N-terminal tail of Rps30/S30e in the body (**Figure 4*c***) (71). Given that mutations in the SI elements reduce start-codon recognition (Ssu$^-$ phenotype), their role in bridging the 40S head and body may underlie their stabilization of the P_{IN} state (76).

Notably, the mRNA entry channel latch is apparently closed in the crystallized mammalian (70) and *Tetrahymena* (71) 40S/eIF1/eIF1A complexes, whereas the cryo-EM model of the analogous yeast complex has an open-latch conformation (186).

Investigators proposed that the latch is closed in the scanning PIC so that mRNA is locked into the binding cleft and the processivity of scanning is increased, whereas the open-latch conformation of the yeast 40S/eIF1/eIF1A complex would facilitate the initial attachment of the 43S PIC to mRNA (70). Another possibility is that, unlike in yeast, eIF3 may be required along with eIF1/eIF1A to open the latch in the mammalian scanning complex. Interestingly, the crystallized mammalian 48S PIC lacks the sharp kink in the mRNA between the A and P sites that is observed in bacterial elongation complexes and is thought to prevent slippage and maintain reading frames during elongation, which may facilitate scanning by the PIC (70).

Movements of the eIF1A-CTT and eIF5-GAP domains stabilize the closed/P_{IN} state and enable phosphate release. An analysis of fluorescently tagged yeIF1A revealed that AUG recognition stabilizes its binding to the PIC and that Sui$^-$ mutations in the eIF1A-CTT or eIF5-GAP domain (*SUI5*) produce the same stabilization at UUG codons (212). Given that Ssu$^-$ mutations in eIF1A-NTT accelerate eIF1A dissociation (75), eIF1A binding affinity may reflect partitioning of the PIC between open and closed conformations. The idea that interaction between eIF5 and eIF1A stabilizes the closed conformation is supported by FRET analyses that indicate movement of eIF5-NTD toward eIF1A-CTT on AUG recognition, which is governed by eIF1 dissociation and depends on the eIF1A SE elements. Remarkably, the SE mutations dramatically impede P_i release and have only modest effects on eIF1 dissociation; these findings suggest that SE-dependent interaction between eIF1A-CTT and eIF5-NTD is required for P_i release following eIF1 dissociation. eIF1 may indirectly impede P_i release at non-AUGs by physically blocking accommodation of Met-tRNA$_i$ in the P site and the attendant movement of eIF1A-CTT toward eIF5 (**Figure 5**). The apparent paradox that SE mutations elevate UUG initiation in vivo while impeding P_i release in vitro might be resolved if the mutations displace the CTT from the P site to an aberrant location that eliminates the CTT clash with Met-tRNA$_i$ and permits rearrangement to the P_{IN} state at UUGs while impairing interaction with eIF5-NTD at AUGs. The interaction between eIF5 and eIF1A may also provoke dissociation of eIF5-GAP from eIF2γ, allowing P_i release from GDP/P_i bound to the G domain (**Figure 5**) (64).

Functions of eIF2 and eIF5 in coupling GTP hydrolysis and phosphate release to AUG recognition. Evidence shows that eIF5-CTD also has a role in stabilizing the closed PIC conformation through its interaction with eIF2β-NTT. eIF1 binds to both eIF5-CTD and eIF2β-NTT in the yeast MFC; these interactions seem to stabilize eIF1 binding to the 40S subunit in the open conformation, given that lethal substitutions in the KH surface of eIF1 weaken the interactions, confer a dominant Sui$^-$ phenotype, and impair eIF1 binding to native PICs (67). However, the addition of excess eIF5-CTD accelerates eIF1 dissociation from yeast PICs (64, 209), indicating that eIF5-CTD plays an opposing role in stabilizing the closed conformation. An NMR analysis of the mammalian factors revealed that binding sites for eIF1 and eIF2β-NTT overlap on eIF5-CTD, and a mutational analysis indicated that interaction with eIF2β-NTT is required specifically for the ability of yeIF5-CTD to enhance eIF1 dissociation. For the mammalian factors, this requirement was attributed to the finding that interaction between eIF5-CTD and either eIF2β-NTT or eIF1 is mutually exclusive (100). For yeast, where this exclusivity does not appear to hold (77), the clash with Met-tRNA$_i$ at AUG may displace eIF1 to an alternative binding site, where its interactions with eIF2β-NTT and eIF5-CTD are weakened (64). This model incorporates the observation that yeIF5-CTD binds directly to the 40S subunit, leading investigators to suggest that movement of eIF1 away from the P site displaces yeIF5-CTD from the 40S in a manner that strengthens the yeIF5-CTD/eIF2β-NTT connection while

weakening eIF1 binding to both factors (**Figure 5**). This hypothesis may explain how an excess of eIF5 accelerates eIF1 release by driving simultaneous eIF5-CTD interactions with eIF2β-NTT and the 40S subunit (64).

Consistent with the ability of excess eIF5 to promote eIF1 dissociation (209), overexpression of eIF5 in mammalian or yeast cells reduces the requirement for an AUG and optimal context for efficient initiation, whereas overexpression of eIF1 has the opposite effect (102, 209, 213–215). These opposing activities are used to negatively autoregulate translation of meIF1 and meIF5, owing to the poor context at the start codons for eIF1 (213, 214) and a uORF that inhibits recognition of the eIF5 AUG codon (215), to achieve an optimal balance between these factors.

Investigators have proposed that optimal context participates with a perfect AUG/AC duplex to stabilize the closed/P_{IN} state (48). Supporting this idea are findings that mutations in yeIF1, yeIF1A, and yeIF2β that increase or decrease usage of UUG codons similarly affect the selection of AUGs in poor context (214). How optimum context is recognized is unknown; however, cross-linking data suggest that the α-subunit of meIF2 approaches the −3 nucleotide (48), and the cryo-EM model of the 43S/Dhx29 complex reveals that meIF2α-I contacts Rps5 in the mRNA exit channel (46). Moreover, an α-less form of eIF2 is less able to discriminate against poor context in reconstituted mammalian PICs (48), implicating eIF2α-I in recognizing optimal context. Apparently, a 5′UTR that is long enough to occupy the mRNA exit channel (~12 nt) is also required to stabilize the closed conformation (126).

In addition to eIF2β-NTT, other domains in eIF2 have been implicated in AUG recognition by isolation of Sui$^-$ mutations (reviewed in Reference 216). These mutations include a substitution (Y142H) in the predicted methionine-binding pocket (217) and sw1 (N135K) of the eIF2γ G domain (**Figure 2*a***), which weaken Met-tRNA$_i$ binding to eIF2 in vitro (23, 218) and, hence, may allow release of Met-tRNA$_i$ into the P site at near-cognate triplets. Other eIF2γ mutations that weaken Met-tRNA$_i$ binding have Ssu$^-$ phenotypes, however, suggesting that the orientation (not simply the affinity) of Met-tRNA$_i$ binding to eIF2 is crucial for initiation accuracy (210). Sui$^-$ mutations in eIF2β (*SUI3-2*/S264Y and L254P) increase GTP hydrolysis by TC in vitro—the same defect reported for the *SUI5* mutation in the eIF5 GAP domain (218); however, whether this defect accelerates gated-P_i release at near-cognate triplets in the PIC is unclear. Because most eIF2β Sui$^-$ mutations map to its ZBD (219), which probably interacts with the eIF2γ G domain (**Figure 2*b***) (39), the affected residues may normally limit GTP hydrolysis or P_i release from the eIF2γ-GTP binding pocket at non-AUGs. Consistent with this idea, Sui$^-$ substitutions in the predicted h1 of yeIF2β (Y131A, S132A), which are expected to anchor this subunit to eIF2γ (**Figure 2**) (38–40), weaken the interaction between eIF2β and eIF2γ (220) and may compromise the putative regulatory function of the ZBD.

The GAP function of eIF5-NTD (221) requires Arg-15, located in the unstructured NTT (222), given that lethal Arg-15 substitutions destroy acceleration of GTP hydrolysis but not eIF5 binding to eIF2 (208, 223, 224). Stabilization of the eIF2-GDP/eIF5 complex by aluminum fluoride (AlF_4^-) is consistent with Arg-15 acting as an "Arg finger" that inserts into the eIF2γ-GTP binding pocket to stabilize the transition state for GTP hydrolysis (224); however, GAP function also strongly depends on PIC assembly (208, 223, 224). Thus, whereas yeIF5 increases the rate of GTP hydrolysis by free TC by ~10^3-fold, the rate increases by ~10^6-fold in 43S PICs reconstituted with eIF1, eIF1A, the TC, and eIF5 (208). TC binding to the PIC may allosterically activate the eIF2γ-GTPase center. An alternative model arose from the finding that eIF5-NTD binds isolated eIF2γ (221) but not eIF2 holoprotein (64). The GTPase center may be sterically occluded in the free TC by eIF2β-ZBD, and the latter may be displaced in the scanning PIC to provide eIF5-NTT with access to the GTP binding

pocket. Subsequent withdrawal of eIF5-NTT from the GTPase center might be required for P_i release on AUG recognition, which could be promoted through interaction between eIF5-NTD and eIF1A-CTT (**Figure 5**) (64).

In yeast reconstituted PICs containing only eIF1, eIF1A, a TC, and eIF5, the rate of GTP hydrolysis differed little between AUG and noncognate triplets in the mRNA, and P_i release was the step most enhanced by AUG recognition (59). In reconstituted mammalian PICs, the rate of GTP hydrolysis was reduced severalfold in the absence of AUG recognition by eIF1 (78) or the combined action of eIF3 and cap-bound eIF4F (225). Although the magnitude of these effects is lower than the acceleration of P_i release evoked by AUG (208), these effects are comparable to differences in P_i release rates between AUG and near cognates such as AUU and UUG in yeast PICs (73, 209). Therefore, an increased rate of GTP hydrolysis evoked by mutations such as *SUI3-2* or *SUI5* (218), or (unknown) physiological regulation of eIF5 or eIF2, may contribute to elevated near-cognate initiation by shifting the equilibrium between eIF2-GTP and eIF2-GDP-P_i farther to the right.

Other preinitation complex components modulate AUG selection. eIF3c-NTD stabilizes the MFC by binding to eIF1 and eIF5-CTD, interactions that also influence start-codon recognition (102). A Sui$^-$ eIF3c-NTD substitution reduces eIF1's association with the MFC and native PICs (107) and probably mimics eIF1 mutations that weaken its 40S binding and occupancy of the scanning PIC (73). A second Sui$^-$ substitution in eIF3c-NTD actually strengthens its interaction with eIF1. This finding led to the proposal that the tighter eIF1/eIF3c-NTD association promotes eIF1 release from the 40S subunit at near-cognate codons (107), which would be consistent with evidence that the 40S and eIF3c-NTD binding surfaces overlap in the α1-helix of eIF1 (67). yeIF4G2 has multiple binding sites for eIF1 in the HEAT domain and the adjacent Arg-rich RNA-binding domain, and mutations in these regions that reduce eIF1 binding confer moderate Sui$^-$ (226) or Ssu$^-$ phenotypes (146). Thus, interactions between eIF4G and eIF1 may also modulate eIF1 binding to the 40S subunit.

A conserved module of yeIF3 composed of eIF3j, the eIF3b RRM, and eIF3a-CTD appears to contact the 40S subunit near the mRNA entry channel (61, 80, 88, 91, 92, 98, 227) and has been implicated in efficient AUG recognition. Mutations that impair interactions between eIF3b-RRM and eIF3j-NTD increase leaky scanning (88, 91, 92), and eIF3a-CTD mutations mask the effects of eIF2β and eIF5 Sui$^-$ mutations in elevating UUG initiation (98). Contacts between this module and the 40S subunit may normally enhance GTP hydrolysis or promote the closed/P_{IN} state at AUG codons. Finally, genetic evidence shows that Ded1, apart from a stimulatory role in scanning (discussed above in the section titled Functions of RNA Helicases in Scanning), promotes AUG recognition by a mechanism that is negatively regulated by Gle1, and hyperactivation of Ded1 apparently reduces the accuracy of initiation (228).

SUBUNIT JOINING AND EUKARYOTIC INITIATION FACTOR RELEASE

Conversion of eIF2 to its GDP-bound state following AUG recognition reduces its affinity for Met-$tRNA_i$ (24) and causes it to dissociate from the 48S PIC in a manner stimulated by the subunit joining factor eIF5B (48). There is evidence that eIF2-GDP leaves the PIC in association with eIF5 and that eIF5 impedes recycling of eIF2-GDP to eIF2-GTP by eIF2B (**Figure 1**) (229, 230). This GDI (GDP dissociation–inhibitory) function involves competition between eIF5-CTD and the linker region of eIF5 and the catalytic domain of eIF2B, eIF2Bε-CTD, for binding to eIF2β-NTT and the eIF2γ G domain, respectively (231). Following eIF2-GDP dissociation, eIF5B-GTP binds to the 40S subunit and accelerates the rate of 60S subunit joining (232, 233).

The structure of aIF5B reveals a four-domain protein (234), of which the G domain and domain II are superimposable on other translation GTPases and domain III is connected to domain IV by a 40-Åhelix (h12). Domain IV interacts with the C-terminal DIDDI residues of eIF1A (235–237); this interaction stimulates eIF5B recruitment to 48S PICs (238) and bulk initiation in yeast cells (235, 239) and accelerates subunit joining and GTP hydrolysis in vitro (232, 233).

Ribosome-stimulated GTP hydrolysis by eIF5B is dispensable for subunit joining (233) but is needed for a functional 80S IC (240–242) because GTP hydrolysis reduces eIF5B affinity for the 80S IC (233) and triggers its release (242). Thus, the deleterious effects of a GTPase-inactivating mutation (T439A) are suppressed by mutations in the G domain or domain II (242), or in 18S rRNA h5 of the 40S subunit (243), that reduce the affinity of eIF5B for ribosomes. The locations of these suppressors fit well with a model of meIF5B/80S complexes derived from DHRC mapping (244), wherein eIF5B occupies a cleft between the two subunits. The G domain sits near the GTPase-activating center of the 60S subunit, domain II interacts with the 40S (including h15), and domain III contacts both subunits. Domain IV may be able to interact with the Acc stem of $tRNA_i$ following eIF2-GDP dissociation. Consistent with this hypothesis, evidence shows that yeIF5B stabilizes Met-$tRNA_i$ binding to 80S ICs (242) in a manner impaired by altering the length or flexibility of the stem (h12) that connects domain IV to the rest of eIF5B (211). Domain IV of bacterial IF2 was proposed to have this function (245), although IF2 affinity for fMet-$tRNA_i$ (246) is much greater than that of eIF5B for Met-$tRNA_i$ (247). GTP hydrolysis and dissociation of eIF5B also stimulate release of eIF1A from the 80S IC, and release depends on the DIDDI motif (**Figure 4*b***) (233, 238). In addition to reducing eIF5B affinity for the ribosome, GTP hydrolysis seems to alter the IC in a way that favors eIF1A release (233, 242).

PROSPECTIVE

The combination of biochemical, structural, and genetic studies conducted during the past decade has increased our understanding of the molecular functions of the initiation factors, their interactions with one another, and the domains and residues that are critical for their activities. This progress, combined with structural analyses of the 80S ribosome and different 40S PICs, plus FRET analyses of interactions between eIF1, -1A, and -5, has enabled the construction of detailed models for the 43S/mRNA PIC and the conformational rearrangements that occur in the transition from scanning to AUG recognition, as well as subunit joining. More discoveries are needed to achieve a complete picture of the myriad connections between factors and the ribosome and of the dynamics of these interactions that occur along the pathway. A thorough understanding of these connections will require high-resolution crystallography and cryo-EM analyses of additional PIC/IC complexes representing different intermediates in the pathway; FRET-based kinetic analyses of conformational rearrangements (including single-molecule studies); and intensive genetic dissection of the factors, ribosomal proteins, and rRNA domains that are central to the initiation process.

Obtaining a high-resolution structure of the eIF3 complex, elucidating the molecular details of its association with other MFC components and the ribosome, and determining its role in 43S PIC attachment to mRNA are all important challenges for the future. Also, it will be critical to understand the mechanism underlying the latent GTPase activity of the TC and its stimulation by eIF5 and other PIC components. All of the interactions involved in recognizing the AUG/AC duplex in the P site and transducing this signal throughout the PIC should be elucidated. It will be particularly interesting to determine the functional importance of rRNA elements in the P site and Met-$tRNA_i$ residues in this process, along with the role of rRNA residues and ribosomal proteins in recognizing the sequence context of the start codon and

influencing transition to the closed/P_{IN} state. It will be important to determine whether mRNA activation and 43S attachment are coupled via activation of the unwinding activities of eIF4F or other helicases by PIC components and to identify the molecular basis for processive, 5′ to 3 directional scanning. The relative importance of the different helicases in scanning versus 43S attachment should be defined by use of genome-wide approaches, such as ribosome profiling (248), so as to identify the importance of each factor for the translation of any given mRNA. A deeper understanding of the basic mechanisms and critical factors in translation initiation will stimulate and enlighten other studies that aim to determine both how translation initiation can be targeted or modified to regulate gene expression in response to external or developmental cues and how defects in this process contribute to human diseases.

DISCLOSURE STATEMENT

The author is not aware of any affiliations, memberships, funding, or financial holdings that might be perceived as affecting the objectivity of this review.

ACKNOWLEDGMENTS

I thank Byung-Sik Shin for the model in **Figure 3*a***, Jon Lorsch and Tom Dever for many helpful discussions and suggestions, and the anonymous expert referees for correcting numerous errors and oversights and for their valuable suggestions for improving the manuscript.

LITERATURE CITED

1. Hinnebusch AG, Dever TE, Asano K. 2007. Mechanism of translation initiation in the yeast *Saccharomyces cerevisiae*. In *Translational Control in Biology and Medicine*, ed. MB Mathews, N Sonenberg, JWB Hershey, pp. 225–68. Cold Spring Harbor, N.Y.: Cold Spring Harb. Lab.
2. Kozak M. 1978. How do eucaryotic ribosomes select initiation regions in messenger RNA? *Cell* 15:1109–23
3. Kozak M. 1979. Inability of circular mRNA to attach to eukaryotic ribosomes. *Nature* 280:82–85
4. Sherman F, Stewart JW. 1982. Mutations altering initiation of translation of yeast iso-1-cytochrome *c*: contrasts between the eukaryotic and prokaryotic initiation process. In *The Molecular Biology of the Yeast* Saccharomyces *Metabolism and Gene Expression*, ed. JN Strathern, EW Jones, JR Broach, pp. 301–34. Cold Spring Harbor, N.Y.: Cold Spring Harb. Lab.
5. Sherman F, Stewart JW, Schweingruber AM. 1980. Mutants of yeast initiating translation of iso-1-cytochrome *c* within a region spanning 37 nucleotides. *Cell* 20:215–22
6. Kozak M. 1984. Selection of initiation sites by eucaryotic ribosomes: effect of inserting AUG triplets upstream from the coding sequence for preproinsulin. *Nucleic Acids Res.* 12:3873–93
7. Kozak M. 1986. Point mutations define a sequence flanking the AUG initiator codon that modulates translation by eukaryotic ribosomes. *Cell* 44:283–92
8. Hinnebusch AG. 2011. Molecular mechanism of scanning and start codon selection in eukaryotes. *Microbiol. Mol. Biol. Rev.* 75:434–67
9. Pelletier J, Sonenberg N. 1985. Insertion mutagenesis to increase secondary structure within the 5′ noncoding region of a eukaryotic mRNA reduces translational efficiency. *Cell* 40:515–26
10. Kozak M. 1986. Influences of mRNA secondary structure on initiation by eukaryotic ribosomes. *Proc. Natl. Acad. Sci. USA* 83:2850–54
11. Pestova TV, Lorsch JR, Hellen CUT. 2007. The mechanism of translation initiation in eukaryotes. In *Translational Control in Biology and Medicine*, ed. MB Mathews, N Sonenberg, JWB Hershey, pp. 87–128. Cold Spring Harbor, N.Y.: Cold Spring Harb. Lab.

12. Lorsch JR, Dever TE. 2010. Molecular view of 43S complex formation and start site selection in eukaryotic translation initiation. *J. Biol. Chem.* 285:21203–7
13. Sonenberg N, Hinnebusch AG. 2009. Regulation of translation initiation in eukaryotes: mechanisms and biological targets. *Cell* 136:731–45
14. Rajyaguru P, Parker R. 2012. RGG motif proteins: modulators of mRNA functional states. *Cell Cycle* 11:2594–99
15. Jackson RJ, Kaminski A, Poyry TAA. 2007. Coupled termination–reinitiation events in mRNA translation. In *Translational Control in Biology and Medicine*, ed. MB Mathews, N Sonenberg, JWB Hershey, pp. 197–224. Cold Spring Harbor, N.Y.: Cold Spring Harb. Lab.
16. Kozak M. 1987. Effects of intercistronic length on the efficiency of reinitiation by eucaryotic ribosomes. *Mol. Cell. Biol.* 7:3438–45
17. Hinnebusch AG. 2005. Translational regulation of GCN4 and the general amino acid control of yeast. *Annu. Rev. Microbiol.* 59:407–50
18. Hinnebusch AG. 2006. eIF3: a versatile scaffold for translation initiation complexes. *Trends Biochem. Sci.* 31:553–62
19. Lawless C, Pearson RD, Selley JN, Smirnova JB, Grant CM, et al. 2009. Upstream sequence elements direct post-transcriptional regulation of gene expression under stress conditions in yeast. *BMC Genomics* 10:7–26
20. Kertesz M, Wan Y, Mazor E, Rinn JL, Nutter RC, et al. 2010. Genome-wide measurement of RNA secondary structure in yeast. *Nature* 467:103–7
21. Doudna JA, Sarnow P. 2007. Translation initiation by viral internal ribosome entry sites. In *Translational Control in Biology and Medicine*, ed. MB Mathews, N Sonenberg, JWB Hershey, pp. 129–54. Cold Spring Harbor, N.Y.: Cold Spring Harb. Lab.
22. Jackson RJ. 2013. The current status of vertebrate cellular mRNA IRESs. *Cold Spring Harb. Perspect. Biol.* 5:a011569
23. Erickson FL, Hannig EM. 1996. Ligand interactions with eukaryotic translation initiation factor 2: role of the γ-subunit. *EMBO J.* 15:6311–20
24. Kapp LD, Lorsch JR. 2004. GTP-dependent recognition of the methionine moiety on initiator tRNA by translation factor eIF2. *J. Mol. Biol.* 335:923–36
25. Wagner T, Gross M, Sigler PB. 1984. Isoleucyl initiator tRNA does not initiate eucaryotic protein synthesis. *J. Biol. Chem.* 259:4706–9
26. Farruggio D, Chaudhuri J, Maitra U, RajBhandary UL. 1996. The A1 × U72 base pair conserved in eukaryotic initiator tRNAs is important specifically for binding to the eukaryotic translation initiation factor eIF2. *Mol. Cell. Biol.* 16:4248–56
27. Kapp LD, Kolitz SE, Lorsch JR. 2006. Yeast initiator tRNA identity elements cooperate to influence multiple steps of translation initiation. *RNA* 12:751–64
28. Astrom SU, von Pawel–Rammingen U, Bystrom AS. 1993. The yeast initiator $tRNA^{Met}$ can act as an elongator $tRNA^{Met}$ in vivo. *J. Mol. Biol.* 233:43–58
29. RajBhandary UL, Chow CM. 1995. Initiator tRNAs and initiation of protein synthesis. In *tRNA Structure, Biosynthesis, and Function*, ed. D Soll, UL RajBhandary, pp. 511–28. Washington, DC: Am. Soc. Microbiol.
30. Benelli D, Londei P. 2011. Translation initiation in Archaea: conserved and domain-specific features. *Biochem. Soc. Trans.* 39:89–93
31. Schmitt E, Blanquet S, Mechulam Y. 2002. The large subunit of initiation factor aIF2 is a close structural homologue of elongation factors. *EMBO J.* 21:1821–32
32. Roll-Mecak A, Alone P, Cao C, Dever TE, Burley SK. 2004. X-ray structure of translation initiation factor eIF2γ: implications for tRNA and eIF2α binding. *J. Biol. Chem.* 279:10634–42
33. Pedullà N, Palermo R, Hasenöhrl D, Bläsi U, Cammarano P, Londei P. 2005. The archaeal eIF2 homologue: functional properties of an ancient translation initiation factor. *Nucleic Acids Res.* 33:1804–12
34. Yatime L, Schmitt E, Blanquet S, Mechulam Y. 2004. Functional molecular mapping of archaeal translation initiation factor 2. *J. Biol. Chem.* 279:15984–93

35. Yatime L, Mechulam Y, Blanquet S, Schmitt E. 2006. Structural switch of the γ subunit in an archaeal aIF2αγ heterodimer. *Structure* 14:119–28
36. Nissen P, Kjeldgaard M, Thirup S, Polekhina G, Reshetnikova L, et al. 1995. Crystal structure of the ternary complex of Phe-tRNA^{Phe}, EF-Tu, and a GTP analog. *Science* 270:1464–72
37. Schmitt E, Panvert M, Lazennec-Schurdevin C, Coureux PD, Perez J, et al. 2012. Structure of the ternary initiation complex aIF2–GDPNP–methionylated initiator tRNA. *Nat. Struct. Mol. Biol.* 19:450–54
38. Sokabe M, Yao M, Sakai N, Toya S, Tanaka I. 2006. Structure of archaeal translational initiation factor 2βγ–GDP reveals significant conformational change of the β-subunit and switch 1 region. *Proc. Natl. Acad. Sci. USA* 103:13016–21
39. Yatime L, Mechulam Y, Blanquet S, Schmitt E. 2007. Structure of an archaeal heterotrimeric initiation factor 2 reveals a nucleotide state between the GTP and the GDP states. *Proc. Natl. Acad. Sci. USA* 104:18445–50
40. Stolboushkina E, Nikonov S, Nikulin A, Bläsi U, Manstein DJ, et al. 2008. Crystal structure of the intact archaeal translation initiation factor 2 demonstrates very high conformational flexibility in the α- and β-subunits. *J. Mol. Biol.* 382:680–91
41. Schmitt E, Naveau M, Mechulam Y. 2010. Eukaryotic and archaeal translation initiation factor 2: a heterotrimeric tRNA carrier. *FEBS Lett.* 584:405–12
42. Nika J, Rippel S, Hannig EM. 2001. Biochemical analysis of the eIF2βγ complex reveals a structural function for eIF2α in catalyzed nucleotide exchange. *J. Biol. Chem.* 276:1051–56
43. Shin BS, Kim JR, Walker SE, Dong J, Lorsch JR, Dever TE. 2011. Initiation factor eIF2 promotes eIF2–GTP–Met-tRNA$_i^{Met}$ ternary complex binding to the 40S ribosome. *Nat. Struct. Mol. Biol.* 18:1227–34
44. Naveau M, Lazennec-Schurdevin C, Panvert M, Dubiez E, Mechulam Y, Schmitt E. 2013. Roles of yeast eIF2α and eIF2β subunits in the binding of the initiator methionyl-tRNA. *Nucleic Acids Res.* 41:1047–57
45. Naveau M, Lazennec-Schurdevin C, Panvert M, Mechulam Y, Schmitt E. 2010. tRNA binding properties of eukaryotic translation initiation factor 2 from *Encephalitozoon cuniculi*. *Biochemistry* 49:8680–88
46. Hashem Y, des Georges A, Dhote V, Langlois R, Liao HY, et al. 2013. Structure of the mammalian ribosomal 43S preinitiation complex bound to the scanning factor DHX29. *Cell* 153:1108–19
47. Ben-Shem A, Garreau de Loubresse N, Melnikov S, Jenner L, Yusupova G, Yusupov M. 2011. The structure of the eukaryotic ribosome at 3.0 Åresolution. *Science* 334:1524–29
48. Pisarev AV, Kolupaeva VG, Pisareva VP, Merrick WC, Hellen CU, Pestova TV. 2006. Specific functional interactions of nucleotides at key −3 and +4 positions flanking the initiation codon with components of the mammalian 48S translation initiation complex. *Genes Dev.* 20:624–36
49. Erickson FL, Nika J, Rippel S, Hannig EM. 2001. Minimum requirements for the function of eukaryotic translation initiation factor 2. *Genetics* 158:123–32
50. Trachsel H, Erni B, Schreier MH, Staehelin T. 1977. Initiation of mammalian protein synthesis: the assembly of the initiation complex with purified initiation factors. *J. Mol. Biol.* 116:755–67
51. Benne R, Hershey JWB. 1978. The mechanism of action of protein synthesis initiation factors from rabbit reticulocytes. *J. Biol. Chem.* 253:3078–87
52. Peterson DT, Merrick WC, Safer B. 1979. Binding and release of radiolabeled eukaroytic initiation factors 2 and 3 during 80 S initiation complex formation. *J. Biol. Chem.* 254:2509–19
53. Thomas A, Spaan W, van Steeg H, Voorma HO, Benne R. 1980. Mode of action of protein synthesis initiation factor eIF-1 from rabbit reticulocytes. *FEBS Lett.* 116:67–71
54. Chaudhuri J, Si K, Maitra U. 1997. Function of eukaryotic translation initiation factor 1A (eIF1A) (formerly called eIF-4C) in initiation of protein synthesis. *J. Biol. Chem.* 272:7883–91
55. Chaudhuri J, Chowdhury D, Maitra U. 1999. Distinct functions of eukaryotic translation initiation factors eIF1A and eIF3 in the formation of the 40S ribosomal preinitiation complex. *J. Biol. Chem.* 274:17975–80
56. Algire MA, Maag D, Savio P, Acker MG, Tarun SZ Jr, et al. 2002. Development and characterization of a reconstituted yeast translation initiation system. *RNA* 8:382–97
57. Majumdar R, Bandyopadhyay A, Maitra U. 2003. Mammalian translation initiation factor eIF1 functions with eIF1A and eIF3 in the formation of a stable 40S preinitiation complex. *J. Biol. Chem.* 278:6580–87

58. Kolupaeva VG, Unbehaun A, Lomakin IB, Hellen CU, Pestova TV. 2005. Binding of eukaryotic initiation factor 3 to ribosomal 40S subunits and its role in ribosomal dissociation and anti-association. *RNA* 11:470–86
59. Maag D, Fekete CA, Gryczynski Z, Lorsch JR. 2005. A conformational change in the eukaryotic translation preinitiation complex and release of eIF1 signal recognition of the start codon. *Mol. Cell* 17:265–75
60. Benne R, Hershey JWB. 1976. Purification and characterization of initiation factor IF-E3 from rabbit reticulocytes. *Proc. Natl. Acad. Sci. USA* 73:3005–9
61. Fraser CS, Lee JY, Mayeur GL, Bushell M, Doudna JA, Hershey JWB. 2004. The j-subunit of human translation initiation factor eIF3 is required for the stable binding of eIF3 and its subcomplexes to 40 S ribosomal subunits in vitro. *J. Biol. Chem.* 279:8946–56
62. Maag D, Lorsch JR. 2003. Communication between eukaryotic translation initiation factors 1 and 1A on the yeast small ribosomal subunit. *J. Mol. Biol.* 330:917–24
63. Sokabe M, Fraser CS, Hershey JWB. 2012. The human translation initiation multi-factor complex promotes methionyl-tRNA$_i$ binding to the 40S ribosomal subunit. *Nucleic Acids Res.* 40:905–13
64. Nanda JS, Saini AK, Munoz AM, Hinnebusch AG, Lorsch JR. 2013. Coordinated movements of eukaryotic translation initiation factors eIF1, eIF1A, and eIF5 trigger phosphate release from eIF2 in response to start codon recognition by the ribosomal preinitiation complex. *J. Biol. Chem.* 288:5316–29
65. Fletcher CM, Pestova TV, Hellen CUT, Wagner G. 1999. Structure and interactions of the translation initiation factor eIF1. *EMBO J.* 18:2631–39
66. Battiste JB, Pestova TV, Hellen CUT, Wagner G. 2000. The eIF1A solution structure reveals a large RNA-binding surface important for scanning function. *Mol. Cell* 5:109–19
67. Reibarkh M, Yamamoto Y, Singh CR, del Rio F, Fahmy A, et al. 2008. Eukaryotic initiation factor (eIF) 1 carries two distinct eIF5-binding faces important for multifactor assembly and AUG selection. *J. Biol. Chem.* 283:1094–103
68. Rabl J, Leibundgut M, Ataide SF, Haag A, Ban N. 2011. Crystal structure of the eukaryotic 40S ribosomal subunit in complex with initiation factor 1. *Science* 331:730–36
69. Yu Y, Marintchev A, Kolupaeva VG, Unbehaun A, Veryasova T, et al. 2009. Position of eukaryotic translation initiation factor eIF1A on the 40S ribosomal subunit mapped by directed hydroxyl radical probing. *Nucleic Acids Res.* 37:5167–82
70. Lomakin IB, Steitz TA. 2013. The initiation of mammalian protein synthesis and mRNA scanning mechanism. *Nature* 500:307–11
71. Weisser M, Voigts-Hoffmann F, Rabl J, Leibundgut M, Ban N. 2013. The crystal structure of the eukaryotic 40S ribosomal subunit in complex with eIF1 and eIF1A. *Nat. Struct. Mol. Biol.* 20:1015–17
72. Lomakin IB, Kolupaeva VG, Marintchev A, Wagner G, Pestova TV. 2003. Position of eukaryotic initiation factor eIF1 on the 40S ribosomal subunit determined by directed hydroxyl radical probing. *Genes Dev.* 17:2786–97
73. Cheung YN, Maag D, Mitchell SF, Fekete CA, Algire MA, et al. 2007. Dissociation of eIF1 from the 40S ribosomal subunit is a key step in start codon selection in vivo. *Genes Dev.* 21:1217–30
74. Fekete CA, Applefield DJ, Blakely SA, Shirokikh N, Pestova T, et al. 2005. The eIF1A C-terminal domain promotes initiation complex assembly, scanning and AUG selection in vivo. *EMBO J.* 24:3588–601
75. Fekete CA, Mitchell SF, Cherkasova VA, Applefield D, Algire MA, et al. 2007. N- and C-terminal residues of eIF1A have opposing effects on the fidelity of start codon selection. *EMBO J.* 26:1602–14
76. Saini AK, Nanda JS, Lorsch JR, Hinnebusch AG. 2010. Regulatory elements in eIF1A control the fidelity of start codon selection by modulating tRNA$_i^{Met}$ binding to the ribosome. *Genes Dev.* 24:97–110
77. Singh CR, He H, Ii M, Yamamoto Y, Asano K. 2004. Efficient incorporation of eukaryotic initiation factor 1 into the multifactor complex is critical for formation of functional ribosomal preinitiation complexes in vivo. *J. Biol. Chem.* 279:31910–20
78. Unbehaun A, Borukhov SI, Hellen CU, Pestova TV. 2004. Release of initiation factors from 48S complexes during ribosomal subunit joining and the link between establishment of codon–anticodon base-pairing and hydrolysis of eIF2-bound GTP. *Genes Dev.* 18:3078–93
79. Phan L, Zhang X, Asano K, Anderson J, Vornlocher HP, et al. 1998. Identification of a translation initiation factor 3 (eIF3) core complex, conserved in yeast and mammals, that interacts with eIF5. *Mol. Cell. Biol.* 18:4935–46

80. Valášek L, Phan L, Schoenfeld LW, Valásková V, Hinnebusch AG. 2001. Related eIF3 subunits TIF32 and HCR1 interact with an RNA recognition motif in PRT1 required for eIF3 integrity and ribosome binding. *EMBO J.* 20:891–904
81. Zhou M, Sandercock AM, Fraser CS, Ridlova G, Stephens E, et al. 2008. Mass spectrometry reveals modularity and a complete subunit interaction map of the eukaryotic translation factor eIF3. *Proc. Natl. Acad. Sci. USA* 105:18139–44
82. Phan L, Schoenfeld LW, Valášek L, Nielsen KH, Hinnebusch AG. 2001. A subcomplex of three eIF3 subunits binds eIF1 and eIF5 and stimulates ribosome binding of mRNA and $tRNA_i^{Met}$. *EMBO J.* 20:2954–65
83. Sun C, Todorovic A, Querol-Audi J, Bai Y, Villa N, et al. 2011. Functional reconstitution of human eukaryotic translation initiation factor 3 (eIF3). *Proc. Natl. Acad. Sci. USA* 108:20473–78
84. Masutani M, Sonenberg N, Yokoyama S, Imataka H. 2007. Reconstitution reveals the functional core of mammalian eIF3. *EMBO J.* 26:3373–83
85. Querol-Audi J, Sun C, Vogan JM, Smith MD, Gu Y, et al. 2013. Architecture of human translation initiation factor 3. *Structure* 6:920–28
86. Siridechadilok B, Fraser CS, Hall RJ, Doudna JA, Nogales E. 2005. Structural roles for human translation factor eIF3 in initiation of protein synthesis. *Science* 310:1513–15
87. Cuchalová L, Kouba T, Herrmannová A, Dányi I, Chiu WL, Valášek L. 2010. The RNA recognition motif of eukaryotic translation initiation factor 3g (eIF3g) is required for resumption of scanning of posttermination ribosomes for reinitiation on GCN4 and together with eIF3i stimulates linear scanning. *Mol. Cell. Biol.* 30:4671–86
88. Elantak L, Wagner S, Herrmannová A, Karásková M, Rutkai E, et al. 2010. The indispensable N-terminal half of eIF3j/HCR1 cooperates with its structurally conserved binding partner eIF3b/PRT1–RRM and with eIF1A in stringent AUG selection. *J. Mol. Biol.* 396:1097–116
89. Herrmannová A, Daujotyte D, Yang JC, Cuchalová L, Gorrec F, et al. 2012. Structural analysis of an eIF3 subcomplex reveals conserved interactions required for a stable and proper translation pre-initiation complex assembly. *Nucleic Acids Res.* 40:2294–311
90. Wei Z, Zhang P, Zhou Z, Cheng Z, Wan M, Gong W. 2004. Crystal structure of human eIF3k, the first structure of eIF3 subunits. *J. Biol. Chem.* 279:34983–90
91. Nielsen KH, Valášek L, Sykes C, Jivotovskaya A, Hinnebusch AG. 2006. Interaction of the RNP1 motif in PRT1 with HCR1 promotes 40S binding of eukaryotic initiation factor 3 in yeast. *Mol. Cell. Biol.* 26:2984–98
92. Elantak L, Tzakos AG, Locker N, Lukavsky PJ. 2007. Structure of eIF3b-RRM and its interaction with eIF3j: structural insights into the recruitment of eIF3b to the 40S ribosomal subunit. *J. Biol. Chem.* 282:8165–74
93. Fraser CS, Berry KE, Hershey JWB, Doudna JA. 2007. eIF3j is located in the decoding center of the human 40S ribosomal subunit. *Mol. Cell* 26:811–19
94. Pisarev AV, Kolupaeva VG, Yusupov MM, Hellen CU, Pestova TV. 2008. Ribosomal position and contacts of mRNA in eukaryotic translation initiation complexes. *EMBO J.* 27:1609–21
95. Ben-Shem A, Jenner L, Yusupova G, Yusupov M. 2010. Crystal structure of the eukaryotic ribosome. *Science* 330:1203–9
96. Valášek L, Mathew A, Shin BS, Nielsen KH, Szamecz B, Hinnebusch AG. 2003. The yeast eIF3 subunits TIF32/a and NIP1/c and eIF5 make critical connections with the 40S ribosome in vivo. *Genes Dev.* 17:786–99
97. Kouba T, Dányi I, Gunisova S, Munzarova V, Vlckova V, et al. 2012. Small ribosomal protein RPS0 stimulates translation initiation by mediating 40S-binding of eIF3 via its direct contact with the eIF3a/TIF32 subunit. *PLoS ONE* 7:e40464
98. Chiu WL, Wagner S, Herrmannová A, Burela L, Zhang F, et al. 2010. The C-terminal region of eukaryotic translation initiation factor 3a (eIF3a) promotes mRNA recruitment, scanning, and, together with eIF3j and the eIF3b RNA recognition motif, selection of AUG start codons. *Mol. Cell. Biol.* 30:4415–34

99. Kouba T, Rutkai E, Karásková M, Valášek L. 2012. The eIF3c/NIP1 PCI domain interacts with RNA and RACK1/ASC1 and promotes assembly of translation preinitiation complexes. *Nucleic Acids Res.* 40:2683–99
100. Luna RE, Arthanari H, Hiraishi H, Nanda J, Martin-Marcos P, et al. 2012. The C-terminal domain of eukaryotic initiation factor 5 promotes start codon recognition by its dynamic interplay with eIF1 and eIF2β. *Cell Rep.* 1:689–702
101. Valášek L, Nielsen KH, Hinnebusch AG. 2002. Direct eIF2–eIF3 contact in the multifactor complex is important for translation initiation in vivo. *EMBO J.* 21:5886–98
102. Valášek L, Nielsen KH, Zhang F, Fekete CA, Hinnebusch AG. 2004. Interactions of eukaryotic translation initiation factor 3 (eIF3) subunit NIP1/c with eIF1 and eIF5 promote preinitiation complex assembly and regulate start codon selection. *Mol. Cell. Biol.* 24:9437–55
103. Asano K, Krishnamoorthy T, Phan L, Pavitt GD, Hinnebusch AG. 1999. Conserved bipartite motifs in yeast eIF5 and eIF2Bε, GTPase-activating and GDP–GTP exchange factors in translation initiation, mediate binding to their common substrate eIF2. *EMBO J.* 18:1673–88
104. Asano K, Clayton J, Shalev A, Hinnebusch AG. 2000. A multifactor complex of eukaryotic initiation factors eIF1, eIF2, eIF3, eIF5, and initiator $tRNA^{Met}$ is an important translation initiation intermediate in vivo. *Genes Dev.* 14:2534–46
105. Singh CR, Yamamoto Y, Asano K. 2004. Physical association of eukaryotic initiation factor (eIF) 5 carboxyl-terminal domain with the lysine-rich eIF2β segment strongly enhances its binding to eIF3. *J. Biol. Chem.* 279:49644–55
106. Yamamoto Y, Singh CR, Marintchev A, Hall NS, Hannig EM, et al. 2005. The eukaryotic initiation factor (eIF) 5 HEAT domain mediates multifactor assembly and scanning with distinct interfaces to eIF1, eIF2, eIF3, and eIF4G. *Proc. Natl. Acad. Sci. USA* 102:16164–69
107. Karásková M, Gunisova S, Herrmannová A, Wagner S, Munzarova V, Valášek L. 2012. Functional characterization of the role of the N-terminal domain of the c/Nip1 subunit of eukaryotic initiation factor 3 (eIF3) in AUG recognition. *J. Biol. Chem.* 287:28420–34
108. Das S, Maiti T, Das K, Maitra U. 1997. Specific interaction of eukaryotic translation initiation factor 5 (eIF5) with the β-subunit of eIF2. *J. Biol. Chem.* 272:31712–18
109. Singh CR, Curtis C, Yamamoto Y, Hall NS, Kruse DS, et al. 2005. Eukaryotic translation initiation factor 5 is critical for integrity of the scanning preinitiation complex and accurate control of GCN4 translation. *Mol. Cell. Biol.* 25:5480–91
110. Jivotovskaya AV, Valášek L, Hinnebusch AG, Nielsen KH. 2006. Eukaryotic translation initiation factor 3 (eIF3) and eIF2 can promote mRNA binding to 40S subunits independently of eIF4G in yeast. *Mol. Cell. Biol.* 26:1355–72
111. Das S, Maitra U. 2000. Mutational analysis of mammalian translation initiation factor 5 (eIF5): role of interaction between the β subunit of eIF2 and eIF5 in eIF5 function in vitro and in vivo. *Mol. Cell. Biol.* 20:3942–50
112. Bieniossek C, Schütz P, Bumann M, Limacher A, Uson I, Baumann U. 2006. The crystal structure of the carboxy-terminal domain of human translation initiation factor eIF5. *J. Mol. Biol.* 360:457–65
113. Dominguez D, Altmann M, Benz J, Baumann U, Trachsel H. 1999. Interaction of translation initiation factor eIF4G with eIF4A in the yeast *Saccharomyces cerevisiae*. *J. Biol. Chem.* 274:26720–26
114. Dominguez D, Kislig E, Altmann M, Trachsel H. 2001. Structural and functional similarities between the central eukaryotic initiation factor (eIF)4A-binding domain of mammalian eIF4G and the eIF4A-binding domain of yeast eIF4G. *Biochem. J.* 355:223–30
115. Imataka H, Sonenberg N. 1997. Human eukaryotic translation initiation factor 4G (eIF4G) possesses two separate and independent binding sites for eIF4A. *Mol. Cell. Biol.* 17:6940–47
116. Neff CL, Sachs AB. 1999. Eukaryotic translation initiation factors eIF4G and eIF4A from *Saccharomyces cerevisiae* physically and functionally interact. *Mol. Cell. Biol.* 19:5557–64
117. Pause A, Méthot N, Svitkin Y, Merrick WC, Sonenberg N. 1994. Dominant negative mutants of mammalian translation initiation factor eIF-4A define a critical role for eIF-4F in cap-dependent and cap-independent initiation of translation. *EMBO J.* 13:1205–15
118. Rogers GW Jr, Komar AA, Merrick WC. 2002. eIF4A: the godfather of the DEAD box helicases. *Prog. Nucleic Acid Res. Mol. Biol.* 72:307–31

119. Schütz P, Bumann M, Oberholzer AE, Bieniossek C, Trachsel H, et al. 2008. Crystal structure of the yeast eIF4A–eIF4G complex: an RNA-helicase controlled by protein–protein interactions. *Proc. Natl. Acad. Sci. USA* 105:9564–69
120. Caruthers JM, Johnson ER, McKay DB. 2000. Crystal structure of yeast initiation factor 4A, a DEAD-box RNA helicase. *Proc. Natl. Acad. Sci. USA* 97:13080–85
121. Oberer M, Marintchev A, Wagner G. 2005. Structural basis for the enhancement of eIF4A helicase activity by eIF4G. *Genes Dev.* 19:2212–23
122. Hilbert M, Kebbel F, Gubaev A, Klostermeier D. 2011. eIF4G stimulates the activity of the DEAD box protein eIF4A by a conformational guidance mechanism. *Nucleic Acids Res.* 39:2260–70
123. Feoktistova K, Tuvshintogs E, Do A, Fraser CS. 2013. Human eIF4E promotes mRNA restructuring by stimulating eIF4A helicase activity. *Proc. Natl. Acad. Sci. USA* 110:13339–44
124. Blum S, Schmid SR, Pause A, Buser P, Linder P, et al. 1992. ATP hydrolysis by initiation factor 4A is required for translation initiation in *Saccharomyces cerevisiae*. *Proc. Natl. Acad. Sci. USA* 89:7664–68
125. Svitkin Y, Pause A, Haghighat A, Pyronnet S, Witherell GW, et al. 2001. The requirement for eukaryotic initiation factor 4A (eIF4A) in translation is in direct proportion to the degree of mRNA 5′ secondary structure. *RNA* 7:382–94
126. Pestova TV, Kolupaeva VG. 2002. The roles of individual eukaryotic translation initiation factors in ribosomal scanning and initiation codon selection. *Genes Dev.* 16:2906–22
127. Mitchell SF, Walker SE, Algire MA, Park EH, Hinnebusch AG, Lorsch JR. 2010. the 5′-7-methylguanosine cap on eukaryotic mRNAs serves both to stimulate canonical translation initiation and block an alternative pathway. *Mol. Cell* 39:950–62
128. Blum S, Schmid SR, Pause A, Buser P, Linder P, et al. 1992. ATP hydrolysis by initiation factor 4A is required for translation initiation in *Saccharomyces cerevisiae*. *Proc. Natl. Acad. Sci. USA* 89:7664–68
129. Park EH, Zhang F, Warringer J, Sunnerhagen P, Hinnebusch AG. 2011. Depletion of eIF4G from yeast cells narrows the range of translational efficiencies genome-wide. *BMC Genomics* 12:1–18
130. Sengoku T, Nureki O, Nakamura A, Kobayashi S, Yokoyama S. 2006. Structural basis for RNA unwinding by the DEAD-box protein *Drosophila* Vasa. *Cell* 125:287–300
131. Liu F, Putnam A, Jankowsky E. 2008. ATP hydrolysis is required for DEAD-box protein recycling but not for duplex unwinding. *Proc. Natl. Acad. Sci. USA* 105:20209–14
132. Parsyan A, Svitkin Y, Shahbazian D, Gkogkas C, Lasko P, et al. 2011. mRNA helicases: the tacticians of translational control. *Nat. Rev. Mol. Cell Biol.* 12:235–45
133. Korneeva NL, Lamphear BJ, Hennigan FL, Rhoads RE. 2000. Mutually cooperative binding of eukaryotic translation initiation factor (eIF) 3 and eIF4A to human eIF4G-1. *J. Biol. Chem.* 275:41369–76
134. LeFebvre AK, Korneeva NL, Trutschl M, Cvek U, Duzan RD, et al. 2006. Translation initiation factor eIF4G-1 binds to eIF3 through the eIF3e subunit. *J. Biol. Chem.* 281:22917–32
135. Marintchev A, Edmonds K, Marintcheva B, Hendrickson E, Oberer M, et al. 2009. Topology and regulation of the human eIF4A/4G/4H helicase complex in translation initiation. *Cell* 136:447–60
136. Asano K, Shalev A, Phan L, Nielsen K, Clayton J, et al. 2001. Multiple roles for the carboxyl terminal domain of eIF5 in translation initiation complex assembly and GTPase activation. *EMBO J.* 20:2326–37
137. Tarun SZ, Wells SE, Deardorff JA, Sachs AB. 1997. Translation initiation factor eIF4G mediates in vitro poly(A) tail–dependent translation. *Proc. Natl. Acad. Sci. USA* 94:9046–51
138. Park E, Walker S, Lee J, Rothenburg S, Lorsch J, Hinnebusch A. 2011. Multiple elements in the eIF4G1 N-terminus promote assembly of eIF4G1 PABP mRNPs in vivo. *EMBO J.* 30:302–16
139. Hinton TM, Coldwell MJ, Carpenter GA, Morley SJ, Pain VM. 2007. Functional analysis of individual binding activities of the scaffold protein eIF4G. *J. Biol. Chem.* 282:1695–708
140. Kahvejian A, Svitkin YV, Sukarieh R, M'Boutchou MN, Sonenberg N. 2005. Mammalian poly(A)-binding protein is a eukaryotic translation initiation factor, which acts via multiple mechanisms. *Genes Dev.* 19:104–13
141. Svitkin YV, Evdokimova VM, Brasey A, Pestova TV, Fantus D, et al. 2009. General RNA-binding proteins have a function in poly(A)-binding protein–dependent translation. *EMBO J.* 28:58–68
142. Yanagiya A, Svitkin YV, Shibata S, Mikami S, Imataka H, Sonenberg N. 2009. Requirement of RNA binding of mammalian eukaryotic translation initiation factor 4GI (eIF4GI) for efficient interaction of eIF4E with the mRNA cap. *Mol. Cell. Biol.* 29:1661–69

143. Arava Y, Wang Y, Storey JD, Liu CL, Brown PO, Herschlag D. 2003. Genome-wide analysis of mRNA translation profiles in *Saccharomyces cerevisiae*. *Proc. Natl. Acad. Sci. USA* 100:3889–94
144. Kaye NM, Emmett KJ, Merrick WC, Jankowsky E. 2009. Intrinsic RNA binding by the eukaryotic initiation factor 4F depends on a minimal RNA length but not on the m^7G cap. *J. Biol. Chem.* 284:17742–50
145. Berset C, Zurbriggen A, Djafarzadeh S, Altmann M, Trachsel H. 2003. RNA-binding activity of translation initiation factor eIF4G1 from *Saccharomyces cerevisiae*. *RNA* 9:871–80
146. Singh CR, Watanabe R, Chowdhury W, Hiraishi H, Murai MJ, et al. 2012. Sequential eukaryotic translation initiation factor 5 (eIF5) binding to the charged disordered segments of eIF4G and eIF2β stabilizes the 48S preinitiation complex and promotes its shift to the initiation mode. *Mol. Cell. Biol.* 32:3978–89
147. Rajagopal V, Park EH, Hinnebusch AG, Lorsch JR. 2012. Specific domains in yeast eIF4G strongly bias the RNA unwinding activity of the eIF4F complex towards duplexes with 5′-overhangs. *J. Biol. Chem.* 287:20301–12
148. Hilliker A, Gao Z, Jankowsky E, Parker R. 2011. The DEAD-box protein Ded1 modulates translation by the formation and resolution of an eIF4F–mRNA complex. *Mol. Cell* 43:962–72
149. Berthelot K, Muldoon M, Rajkowitsch L, Hughes J, McCarthy JE. 2004. Dynamics and processivity of 40S ribosome scanning on mRNA in yeast. *Mol. Microbiol.* 51:987–1001
150. Abaeva IS, Marintchev A, Pisareva VP, Hellen CU, Pestova TV. 2011. Bypassing of stems versus linear base-by-base inspection of mammalian mRNAs during ribosomal scanning. *EMBO J.* 30:115–29
151. Rozovsky N, Butterworth AC, Moore MJ. 2008. Interactions between eIF4AI and its accessory factors eIF4B and eIF4H. *RNA* 14:2136–48
152. Dmitriev SE, Terenin IM, Dunaevsky YE, Merrick WC, Shatsky IN. 2003. Assembly of 48S translation initiation complexes from purified components with mRNAs that have some base pairing within their 5′ untranslated regions. *Mol. Cell. Biol.* 23:8925–33
153. Shahbazian D, Parsyan A, Petroulakis E, Topisirovic I, Martineau Y, et al. 2010. Control of cell survival and proliferation by mammalian eukaryotic initiation factor 4B. *Mol. Cell. Biol.* 30:1478–85
154. Bi X, Ren J, Goss DJ. 2000. Wheat germ translation initiation factor eIF4B affects eIF4A and eIFiso4F helicase activity by increasing the ATP binding affinity of eIF4A. *Biochemistry* 39:5758–65
155. Nielsen KH, Behrens MA, He Y, Oliveira CL, Jensen LS, et al. 2011. Synergistic activation of eIF4A by eIF4B and eIF4G. *Nucleic Acids Res.* 39:2678–89
156. Ozes AR, Feoktistova K, Avanzino BC, Fraser CS. 2011. Duplex unwinding and ATPase activities of the DEAD-box helicase eIF4A are coupled by eIF4G and eIF4B. *J. Mol. Biol.* 412:674–87
157. Altmann M, Wittmer B, Méthot N, Sonenberg N, Trachsel H. 1995. The *Saccharomyces cerevisiae* translation initiation factor Tif3 and its mammalian homologue, eIF-4B, have RNA annealing activity. *EMBO J.* 14:3820–27
158. Altmann M, Müller PP, Wittmer B, Ruchti F, Lanker S, Trachsel H. 1993. A *Saccharomyces cerevisiae* homologue of mammalian translation initiation factor 4B contributes to RNA helicase activity. *EMBO J.* 12:3997–4003
159. Coppolecchia R, Buser P, Stotz A, Linder P. 1993. A new yeast translation initiation factor suppresses a mutation in the eIF-4A RNA helicase. *EMBO J.* 12:4005–11
160. Walker SE, Zhou F, Mitchell SF, Larson VS, Valášek L, et al. 2013. Yeast eIF4B binds to the head of the 40S ribosomal subunit and promotes mRNA recruitment through its N-terminal and internal repeat domains. *RNA* 19:191–207
161. Andreou AZ, Klostermeier D. 2014. eIF4B and eIF4G jointly stimulate eIF4A ATPase and unwinding activities by modulation of the eIF4A conformational cycle. *J. Mol. Biol.* 4261:51–61
162. Park EH, Walker SE, Zhou F, Lee JM, Rajagopal V, et al. 2012. Yeast eukaryotic initiation factor (eIF) 4B enhances complex assembly between eIF4A and eIF4G in vivo. *J. Biol. Chem.* 288:2340–54
163. Méthot N, Song MS, Sonenberg N. 1996. A region rich in aspartic acid, arginine, tyrosine, and glycine (DRYFG) mediates eukaryotic initiation factor 4B (eIF4B) self-association and interaction with eIF3. *Mol. Cell. Biol.* 16:5328–34

164. Méthot N, Pickett G, Keene JD, Sonenberg N. 1996. In vitro RNA selection identifies RNA ligands that specifically bind to eukaryotic translation initiation factor 4B: the role of the RNA remotif. *RNA* 2:38–50
165. Vassilenko KS, Alekhina OM, Dmitriev SE, Shatsky IN, Spirin AS. 2011. Unidirectional constant rate motion of the ribosomal scanning particle during eukaryotic translation initiation. *Nucleic Acids Res.* 39:5555–67
166. Matsuda D, Dreher TW. 2006. Close spacing of AUG initiation codons confers dicistronic character on a eukaryotic mRNA. *RNA* 12:1338–49
167. Prévôt D, Décimo D, Herbreteau CH, Roux F, Garin J, et al. 2003. Characterization of a novel RNA-binding region of eIF4GI critical for ribosomal scanning. *EMBO J.* 22:1909–21
168. Watanabe R, Murai MJ, Singh CR, Fox S, Ii M, Asano K. 2010. The eukaryotic initiation factor (eIF) 4G HEAT domain promotes translation re-initiation in yeast both dependent on and independent of eIF4A mRNA helicase. *J. Biol. Chem.* 285:21922–33
169. Kozak M. 1977. Nucleotide sequences of 5′-terminal ribosome–protected initiation regions from two reovirus messages. *Nature* 269:391–94
170. Lazarowitz SG, Robertson HD. 1977. Initiator regions from the small size class of reovirus messenger RNA protected by rabbit reticulocyte ribosomes. *J. Biol. Chem.* 252:7842–49
171. Spirin AS. 2009. How does a scanning ribosomal particle move along the 5′-untranslated region of eukaryotic mRNA? Brownian ratchet model. *Biochemistry* 48:10688–92
172. Niederberger N, Trachsel H, Altmann M. 1998. The RNA recognition motif of yeast translation initiation factor Tif3/eIF4B is required but not sufficient for RNA strand-exchange and translational activity. *RNA* 4:1259–67
173. Pisareva VP, Pisarev AV, Komar AA, Hellen CU, Pestova TV. 2008. Translation initiation on mammalian mRNAs with structured 5′UTRs requires DExH-box protein DHX29. *Cell* 135:1237–50
174. Dhote V, Sweeney TR, Kim N, Hellen CU, Pestova TV. 2012. Roles of individual domains in the function of DHX29, an essential factor required for translation of structured mammalian mRNAs. *Proc. Natl. Acad. Sci. USA* 109:E3150–59
175. Parsyan A, Shahbazian D, Martineau Y, Petroulakis E, Alain T, et al. 2009. The helicase protein DHX29 promotes translation initiation, cell proliferation, and tumorigenesis. *Proc. Natl. Acad. Sci. USA* 106:22217–22
176. Chuang RY, Weaver PL, Liu Z, Chang TH. 1997. Requirement of the DEAD-box protein ded1p for messenger RNA translation. *Science* 275:1468–71
177. de la Cruz J, Iost I, Kressler D, Linder P. 1997. The p20 and Ded1 proteins have antagonistic roles in eIF4E-dependent translation in *Saccharomyces cerevisiae*. *Proc. Natl. Acad. Sci. USA* 94:5201–6
178. Jamieson DJ, Beggs JD. 1991. A suppressor of yeast spp81/ded1 mutations encodes a very similar putative ATP-dependent RNA helicase. *Mol. Microbiol.* 5:805–12
179. Marsden S, Nardelli M, Linder P, McCarthy JE. 2006. Unwinding single RNA molecules using helicases involved in eukaryotic translation initiation. *J. Mol. Biol.* 361:327–35
180. Lai MC, Lee YH, Tarn WY. 2008. The DEAD-box RNA helicase DDX3 associates with export messenger ribonucleoproteins as well as tip-associated protein and participates in translational control. *Mol. Biol. Cell* 19:3847–58
181. Soto-Rifo R, Rubilar PS, Limousin T, de Breyne S, Décimo D, Ohlmann T. 2012. DEAD-box protein DDX3 associates with eIF4F to promote translation of selected mRNAs. *EMBO J.* 31:3745–56
182. Lee CS, Dias AP, Jedrychowski M, Patel AH, Hsu JL, Reed R. 2008. Human DDX3 functions in translation and interacts with the translation initiation factor eIF3. *Nucleic Acids Res.* 36:4708–18
183. Geissler R, Golbik RP, Behrens SE. 2012. The DEAD-box helicase DDX3 supports the assembly of functional 80S ribosomes. *Nucleic Acids Res.* 40:4998–5011
184. Cigan AM, Feng L, Donahue TF. 1988. $tRNA_i^{Met}$ functions in directing the scanning ribosome to the start site of translation. *Science* 242:93–97
185. Kolitz SE, Takacs JE, Lorsch JR. 2009. Kinetic and thermodynamic analysis of the role of start codon/anticodon base pairing during eukaryotic translation initiation. *RNA* 15:138–52
186. Passmore LA, Schmeing TM, Maag D, Applefield DJ, Acker MG, et al. 2007. The eukaryotic translation initiation factors eIF1 and eIF1A induce an open conformation of the 40S ribosome. *Mol. Cell* 26:41–50

187. Lin CA, Ellis SR, True HL. 2009. The Sua5 protein is essential for normal translational regulation in yeast. *Mol. Cell. Biol.* 30:354–63
188. El Yacoubi B, Lyons B, Cruz Y, Reddy R, Nordin B, et al. 2009. The universal YrdC/Sua5 family is required for the formation of threonylcarbamoyladenosine in tRNA. *Nucleic Acids Res.* 37:2894–909
189. Daugeron MC, Lenstra TL, Frizzarin M, El Yacoubi B, Liu X, et al. 2011. Gcn4 misregulation reveals a direct role for the evolutionary conserved EKC/KEOPS in the t6A modification of tRNAs. *Nucleic Acids Res.* 39:6148–60
190. Srinivasan M, Mehta P, Yu Y, Prugar E, Koonin EV, et al. 2011. The highly conserved KEOPS/EKC complex is essential for a universal tRNA modification, t6A. *EMBO J.* 30:873–81
191. El Yacoubi B, Hatin I, Deutsch C, Kahveci T, Rousset JP, et al. 2011. A role for the universal Kae1/Qri7/YgjD (COG0533) family in tRNA modification. *EMBO J.* 30:882–93
192. Korostelev A, Trakhanov S, Laurberg M, Noller HF. 2006. Crystal structure of a 70S ribosome–tRNA complex reveals functional interactions and rearrangements. *Cell* 126:1065–77
193. Selmer M, Dunham CM, Murphy FV IV, Weixlbaumer A, Petry S, et al. 2006. Structure of the 70S ribosome complexed with mRNA and tRNA. *Science* 313:1935–42
194. Simonetti A, Marzi S, Myasnikov AG, Fabbretti A, Yusupov M, et al. 2008. Structure of the 30S translation initiation complex. *Nature* 455:416–20
195. Dong J, Nanda JS, Rahman H, Pruitt MR, Shin BS, et al. 2008. Genetic identification of yeast 18S rRNA residues required for efficient recruitment of initiator $tRNA^{Met}$ and AUG selection. *Genes Dev.* 22:2242–55
196. Nemoto N, Singh CR, Udagawa T, Wang S, Thorson E, et al. 2010. Yeast 18 S rRNA is directly involved in the ribosomal response to stringent AUG selection during translation initiation. *J. Biol. Chem.* 285:32200–12
197. Lancaster L, Noller HF. 2005. Involvement of 16S rRNA nucleotides G1338 and A1339 in discrimination of initiator tRNA. *Mol. Cell* 20:623–32
198. Abdi NM, Fredrick K. 2005. Contribution of 16S rRNA nucleotides forming the 30S subunit A and P sites to translation in *Escherichia coli*. *RNA* 11:1624–32
199. Qin D, Abdi NM, Fredrick K. 2007. Characterization of 16S rRNA mutations that decrease the fidelity of translation initiation. *RNA* 13:2348–55
200. Drabkin HJ, Helk B, RajBhandary UL. 1993. The role of nucleotides conserved in eukaryotic initiator methionine tRNAs in initiation of protein synthesis. *J. Biol. Chem.* 268:25221–28
201. Lomakin IB, Shirokikh NE, Yusupov MM, Hellen CU, Pestova TV. 2006. The fidelity of translation initiation: reciprocal activities of eIF1, IF3 and YciH. *EMBO J.* 25:196–210
202. von Pawel–Rammingen U, Åström S, Byström AS. 1992. Mutational analysis of conserved positions potentially important for initiator tRNA function in *Saccharomyces cerevisiae*. *Mol. Cell. Biol.* 12:1432–42
203. Battle DJ, Doudna JA. 2002. Specificity of RNA–RNA helix recognition. *Proc. Natl. Acad. Sci. USA* 99:11676–81
204. Basavappa R, Sigler PB. 1991. The 3 Åcrystal structure of yeast initiator tRNA: functional implications in initiator/elongator discrimination. *EMBO J.* 10:3105–11
205. Schmeing TM, Voorhees RM, Kelley AC, Ramakrishnan V. 2011. How mutations in tRNA distant from the anticodon affect the fidelity of decoding. *Nat. Struct. Mol. Biol.* 18:432–36
206. Pestova TV, Borukhov SI, Hellen CUT. 1998. Eukaryotic ribosomes require initiation factors 1 and 1A to locate initiation codons. *Nature* 394:854–59
207. Yoon HJ, Donahue TF. 1992. The *sui1* suppressor locus in *Saccharomyces cerevisiae* encodes a translation factor that functions during $tRNA_i^{Met}$ recognition of the start codon. *Mol. Cell. Biol.* 12:248–60
208. Algire MA, Maag D, Lorsch JR. 2005. Pi release from eIF2, not GTP hydrolysis, is the step controlled by start-site selection during eukaryotic translation initiation. *Mol. Cell* 20:251–62
209. Nanda JS, Cheung YN, Takacs JE, Martin-Marcos P, Saini AK, et al. 2009. eIF1 controls multiple steps in start codon recognition during eukaryotic translation initiation. *J. Mol. Biol.* 394:268–85
210. Alone PV, Cao C, Dever TE. 2008. Translation initiation factor 2γ mutant alters start codon selection independent of Met-tRNA binding. *Mol. Cell. Biol.* 28:6877–88
211. Shin BS, Acker MG, Kim JR, Maher KN, Arefin SM, et al. 2011. Structural integrity of α-helix H12 in translation initiation factor eIF5B is critical for 80S complex stability. *RNA* 17:687–96

212. Maag D, Algire MA, Lorsch JR. 2006. Communication between eukaryotic translation initiation factors 5 and 1A within the ribosomal pre-initiation complex plays a role in start site selection. *J. Mol. Biol.* 356:724–37
213. Ivanov IP, Loughran G, Sachs MS, Atkins JF. 2010. Initiation context modulates autoregulation of eukaryotic translation initiation factor 1 (eIF1). *Proc. Natl. Acad. Sci. USA* 107:18056–60
214. Martin-Marcos P, Cheung YN, Hinnebusch AG. 2011. Functional elements in initiation factors 1, 1A and 2β discriminate against poor AUG context and non-AUG start codons. *Mol. Cell. Biol.* 31:4814–31
215. Loughran G, Sachs MS, Atkins JF, Ivanov IP. 2012. Stringency of start codon selection modulates autoregulation of translation initiation factor eIF5. *Nucleic Acids Res.* 40:2898–906
216. Donahue T. 2000. Genetic approaches to translation initiation in *Saccharomyces cerevisiae*. In *Translational Control of Gene Expression*, ed. N Sonenberg, JWB Hershey, MB Mathews, pp. 487–502. Cold Spring Harbor, N.Y.: Cold Spring Harb. Lab.
217. Dorris DR, Erickson FL, Hannig EM. 1995. Mutations in *GCD11*, the structural gene for eIF-2γ in yeast, alter translational regulation of *GCN4* and the selection of the start site for protein synthesis. *EMBO J.* 14:2239–49
218. Huang H, Yoon H, Hannig EM, Donahue TF. 1997. GTP hydrolysis controls stringent selection of the AUG start codon during translation initiation in *Saccharomyces cerevisiae*. *Genes Dev.* 11:2396–413
219. Donahue TF, Cigan AM, Pabich EK, Castilho-Valavicius B. 1988. Mutations at a Zn(II) finger motif in the yeast eIF-2β gene alter ribosomal start-site selection during the scanning process. *Cell* 54:621–32
220. Hashimoto NN, Carnevalli LS, Castilho BA. 2002. Translation initiation at non-AUG codons mediated by weakened association of eukaryotic initiation factor (eIF) 2 subunits. *Biochem. J.* 367:359–68
221. Alone PV, Dever TE. 2006. Direct binding of translation initiation factor eIF2γ–G domain to its GTPase-activating and GDP–GTP exchange factors eIF5 and eIF2Bε. *J. Biol. Chem.* 281:12636–44
222. Conte MR, Kelly G, Babon J, Sanfelice D, Youell J, et al. 2006. Structure of the eukaryotic initiation factor (eIF) 5 reveals a fold common to several translation factors. *Biochemistry* 45:4550–58
223. Das S, Ghosh R, Maitra U. 2001. Eukaryotic translation initiation factor 5 functions as a GTPase-activating protein. *J. Biol. Chem.* 276:6720–26
224. Paulin FE, Campbell LE, O'Brien K, Loughlin J, Proud CG. 2001. Eukaryotic translation initiation factor 5 (eIF5) acts as a classical GTPase-activator protein. *Curr. Biol.* 11:55–59
225. Majumdar R, Maitra U. 2005. Regulation of GTP hydrolysis prior to ribosomal AUG selection during eukaryotic translation initiation. *EMBO J.* 24:3737–46
226. He H, von der Haar T, Singh CR, Ii M, Li B, et al. 2003. The yeast eukaryotic initiation factor 4G (eIF4G) HEAT domain interacts with eIF1 and eIF5 and is involved in stringent AUG selection. *Mol. Cell. Biol.* 23:5431–45
227. Evans DR, Rasmussen C, Hanic-Joyce PJ, Johnston GC, Singer RA, Barnes CA. 1995. Mutational analysis of the Prt1 protein subunit of yeast translation initiation factor 3. *Mol. Cell. Biol.* 15:4525–35
228. Bolger TA, Wente SR. 2011. Gle1 is a multifunctional DEAD-box protein regulator that modulates Ded1 in translation initiation. *J. Biol. Chem.* 286:39750–59
229. Singh CR, Lee B, Udagawa T, Mohammad-Qureshi SS, Yamamoto Y, et al. 2006. An eIF5/eIF2 complex antagonizes guanine nucleotide exchange by eIF2B during translation initiation. *EMBO J.* 25:4537–46
230. Singh CR, Udagawa T, Lee B, Wassink S, He H, et al. 2007. Change in nutritional status modulates the abundance of critical pre-initiation intermediate complexes during translation initiation in vivo. *J. Mol. Biol.* 370:315–30
231. Jennings MD, Pavitt GD. 2010. eIF5 has GDI activity necessary for translational control by eIF2 phosphorylation. *Nature* 465:378–81
232. Acker MG, Shin BS, Dever TE, Lorsch JR. 2006. Interaction between eukaryotic initiation factors 1A and 5B is required for efficient ribosomal subunit joining. *J. Biol. Chem.* 281:8469–75
233. Acker MG, Shin BS, Nanda JS, Saini AK, Dever TE, Lorsch JR. 2009. Kinetic analysis of late steps of eukaryotic translation initiation. *J. Mol. Biol.* 385:491–506
234. Roll-Mecak A, Cao C, Dever TE, Burley SK. 2000. X-ray structures of the universal translation initiation factor IF2/eIF5B. Conformational changes on GDP and GTP binding. *Cell* 103:781–92

235. Choi SK, Olsen DS, Roll-Mecak A, Martung A, Remo KL, et al. 2000. Physical and functional interaction between the eukaryotic orthologs of prokaryotic translation initiation factors IF1 and IF2. *Mol. Cell. Biol.* 20:7183–91
236. Olsen DS, Savner EM, Mathew A, Zhang F, Krishnamoorthy T, et al. 2003. Domains of eIF1A that mediate binding to eIF2, eIF3 and eIF5B and promote ternary complex recruitment in vivo. *EMBO J.* 22:193–204
237. Marintchev A, Kolupaeva VG, Pestova TV, Wagner G. 2003. Mapping the binding interface between human eukaryotic initiation factors 1A and 5B: a new interaction between old partners. *Proc. Natl. Acad. Sci. USA* 100:1535–40
238. Fringer JM, Acker MG, Fekete CA, Lorsch JR, Dever TE. 2007. Coupled release of eukaryotic translation initiation factors 5B and 1A from 80S ribosomes following subunit joining. *Mol. Cell. Biol.* 27:2384–97
239. Kainuma M, Hershey JWB. 2001. Depletion and deletion analyses of eucaryotic translation initiation factor 1A *Sacchaaromyces cerevisiae*. *Biochimie* 83:505–14
240. Pestova TV, Lomakin IB, Lee JH, Choi SK, Dever TE, Hellen CUT. 2000. The joining of ribosomal subunits in eukaryotes requires eIF5B. *Nature* 403:332–35
241. Lee JH, Pestova TV, Shin BS, Cao C, Choi SK, Dever TE. 2002. Initiation factor eIF5B catalyzes second GTP-dependent step in eukaryotic translation initiation. *Proc. Natl. Acad. Sci. USA* 99:16689–94
242. Shin BS, Maag D, Roll-Mecak A, Arefin MS, Burley SK, et al. 2002. Uncoupling of initiation factor eIF5B/IF2 GTPase and translational activities by mutations that lower ribosome affinity. *Cell* 111:1015–25
243. Shin BS, Kim JR, Acker MG, Maher KN, Lorsch JR, Dever TE. 2009. rRNA suppressor of a eukaryotic translation initiation factor 5B/initiation factor 2 mutant reveals a binding site for translational GTPases on the small ribosomal subunit. *Mol. Cell. Biol.* 29:808–21
244. Unbehaun A, Marintchev A, Lomakin IB, Didenko T, Wagner G, et al. 2007. Position of eukaryotic initiation factor eIF5B on the 80S ribosome mapped by directed hydroxyl radical probing. *EMBO J.* 26:3109–23
245. Allen GS, Zavialov A, Gursky R, Ehrenberg M, Frank J. 2005. The cryo-EM structure of a translation initiation complex from *Escherichia coli*. *Cell* 121:703–12
246. Guenneugues M, Caserta E, Brandi L, Spurio R, Meunier S, et al. 2000. Mapping the fMet-tRNA^{fMet} binding site of initiation factor IF2. *EMBO J.* 19:5233–40
247. Guillon L, Schmitt E, Blanquet S, Mechulam Y. 2005. Initiator tRNA binding by e/aIF5B, the eukaryotic/archaeal homologue of bacterial initiation factor IF2. *Biochemistry* 44:15594–601
248. Ingolia NT, Ghaemmaghami S, Newman JR, Weissman JS. 2009. Genome-wide analysis in vivo of translation with nucleotide resolution using ribosome profiling. *Science* 324:218–23